

1 **Estimating pasture quality of Mediterranean grasslands using hyperspectral**
2 **narrow bands from field spectroscopy by Random Forest and PLS regressions**

3 Jesús Fernández-Habas^a, Mónica Carriere Cañada^a, Alma María García Moreno^a, José
4 Ramón Leal-Murillo^a, María P González-Dugo^b, Begoña Abellanas Oar^a, Pedro J.
5 Gómez-Giráldez^b, Pilar Fernández-Rebollo^a

6
7 ^a Department of Forest Engineering, ETSIAM, University of Cordoba, Ctra. Madrid,
8 Km 396. 14071 Córdoba, Spain.

9 ^bIFAPA, Institute of Agricultural and Fisheries Research and Training of Andalusia,
10 Avd. Menéndez Pidal s/n, 14071 Cordoba, Spain.

11
12 **Abstract**

13 Mediterranean grasslands are a cornerstone ecosystem to provide ecosystem services
14 and sustain human societies. The sustainability and provision of ecosystem services by
15 these systems rely on their management. One of the main attributes to perform
16 sustainable and effective management is pasture quality, which is crucial for animal
17 performance in rainfed extensive systems. Remote sensing of grasslands can be an
18 effective tool to inform the management of grasslands. The forthcoming high-priority
19 mission candidate of the European Space Agency, Copernicus Hyperspectral Imaging
20 Mission for the Environment (CHIME) with continuous narrow bands of ≥ 10 nm
21 spectral resolution could be an asset to provide accurate information on the pasture
22 quality of high-diverse and heterogeneous grasslands. In this study, we investigated the
23 potential of CHIME-like field spectroscopy data at 10 nm resolution to assess the
24 quality of Mediterranean permanent grasslands. The pasture quality indicators used
25 were: crude protein (CP), neutral detergent fibre (NDF), acid detergent fibre (ADF) and
26 enzyme digestibility of organic matter (EDOM). To do so, two machine learning
27 methods commonly used in remote sensing were implemented: Partial Least Squares
28 (PLS) regression and Random Forest (RF) regression. The results using all bands in the
29 400-2300 nm spectral range and the results obtained by Backward Feature Elimination

30 (BFE) were also compared. Finally, using importance measures of PLS and RF and the
31 BFE approach, the importance and stability of the bands to assess the pasture quality
32 indicators were explored. The results showed that field spectroscopy CHIME-like data
33 at 10 nm of spectral resolution show potential to predict CP at “good” accuracy and
34 NDF at “moderate” accuracy level in Mediterranean permanent grasslands. PLS
35 outperformed RF to predict CP and NDF in terms of accuracy and certainty of the
36 predictions. The BFE approach increased the accuracy of the predictions, especially in
37 PLS, for which a $\Delta\text{RMSE} = -12.5$ was achieved in cross-validation to predict CP. The
38 models built by BFE approach to predict CP using PLS provided a mean R^2 value of
39 0.82 and a range of 0.68-0.90 in bootstrapped predictions. The RMSE was low (mean
40 $\text{RMSE} = 2.23\%$) and the mean $\text{RPD} = 2.47$ with values ranging from 1.81 to 3.23. RF
41 models to predict CP produced mean R^2 value of 0.68, mean $\text{RMSE} = 3.00\%$ and mean
42 $\text{RPD} = 1.82$. ADF and EDOM were predicted with poor accuracy and similarly by both,
43 PLS and RF. The bands located in the red-edge and NIR region showed high
44 importance and stability to assess the best-predicted variables. Bands centred at 700,
45 710, 1160, 1170 and 1180 are highly stable and important to predict CP. The bands
46 from the SWIR region had lower stability. This study provides insightful results on the
47 use of hyperspectral data and future satellite missions such as CHIME to assess the
48 pasture quality of Mediterranean grasslands that can be crucial to inform the
49 management and monitoring of Mediterranean permanent grasslands.

50 **Keywords:** Crude protein, Band selection, Backward feature elimination, CHIME,
51 Band importance, Heterogeneity

52

53 **1. Introduction**

54 The high diversity of vascular plants, strongly related to the management practices and
55 characteristics of the Mediterranean climate, make the Mediterranean Basin a global

56 biodiversity hotspot (Cosentino et al., 2014; Myers et al., 2000). Grasslands of the
57 Mediterranean-climate zones contribute substantially to the biodiversity of the
58 Mediterranean Basin and have traditionally played a major role to sustain human
59 livelihood (Jouven et al., 2010; Porqueddu et al., 2016). Mediterranean grasslands are
60 mainly annual high-diverse communities of grasses, legumes and forbs, of low biomass
61 production due to the low rainfall and its high intra- and inter-annual variability which
62 together with the grazing and occasional cropping are responsible for the strong
63 heterogeneity of this ecosystem (Cosentino et al., 2014; Olea and San Miguel-Ayanz,
64 2006; Porqueddu et al., 2016). In the last decades, increasing attention has been directed
65 to the potential of Mediterranean grasslands ecosystems to provide multiple ecosystem
66 services highly appreciated by the society and of crucial importance for the global
67 environment such as biodiversity conservation, wildfires control and rural population
68 sustain (D'Ottavio et al., 2018; Porqueddu et al., 2016; Porqueddu et al., 2017).

69 Mediterranean grasslands are associated with extensive livestock grazing by small
70 ruminants and beef cattle (Cosentino et al., 2014) that act as a major driver determining
71 stability, sustainability, and potential of ecosystem services provision (D'Ottavio et al.,
72 2018; Porqueddu et al., 2017; Sollenberger et al., 2019). The increasing effects of
73 climate change challenge the stability and functions of Mediterranean grasslands
74 compromising their resilience (Giannakopoulos et al., 2009; Giorgi and Lionello, 2008;
75 Chang et al., 2017; Ma et al., 2017, Carpintero et al., 2020). In this context, it is crucial
76 to have accurate and routine information on the attributes of grasslands to i) improve the
77 economic, environmental sustainability and efficiency of grassland management at farm
78 level, and ii) monitor their dynamics and conservation status at a larger scale. One of the
79 most important attributes of grasslands concerning their management for livestock
80 rearing is the pasture quality. Pasture's quality can be understood in many ways, but in

81 the context of animal feeding, it usually refers to proximate nutritional principles
82 (Dumont et al., 2015) such as crude protein and fibre, ether extract, minerals, ash, or the
83 energy provided (Pullanagari et al., 2013).

84 The main methods to assess pasture quality are: i) laboratory-based methods, ii)
85 proximal remote sensing, iii) aerial remote sensing (aircrafts and UAVs) and iv) space-
86 based remote sensing (Pullanagari et al., 2013). The accuracy of the estimations is
87 reduced following the order in which these methods have been listed (Pullanagari et al.,
88 2013). Laboratory-based methods are the standard and commonly used ~~methods~~ to
89 assess pasture quality. However, through the previous calibration using reference data
90 determined by laboratory methods, indirect methods based on the remote sensing of the
91 pasture reflectance are gaining importance in pasture quality determination. Concerning
92 the cost, laboratory-based methods are the most expensive methods due to laborious
93 manual sampling collection and analysis compared to the sensing methods (Starks et al.,
94 2004). Within the sensing methods, satellite technology is especially interesting because
95 of the large-scale coverage and regular data provision. In particular, Sentinel-2 satellites
96 have demonstrated a great potential to monitor grasslands ecosystems (Askari et al.,
97 2019; Fernández-Habas et al., 2021; Raab et al., 2020; Ramoelo et al., 2014; Sibanda et
98 al., 2015) due to the free provision of multispectral data at worldwide level with a
99 frequency of 5 days (ESA, 2021). However, because of the intrinsic heterogeneity of
100 Mediterranean grasslands, multispectral data might have limited potential to provide
101 accurate information on quality grasslands attributes (Fernández-Habas et al., 2021).
102 The European Space Agency has a new high-priority mission candidate Copernicus
103 Hyperspectral Imaging Mission for the Environment (CHIME) (Nieke and Rast, 2018;
104 Rast et al., 2019). The objective of this mission is: *“To provide routine hyperspectral
105 observations through the Copernicus Programme in support of EU- and related policies*

106 *for the management of natural resources, assets and benefits*". According to the
107 Mission Requirements Document, this imaging spectrometer will measure in the 400-
108 2500 nm spectral range with continuous narrow bands of ≥ 10 nm spectral resolution,
109 spatial resolution of 20-30 m and revisiting time of 10 to 12.5 days (Nieke and Rast,
110 2018; Rast et al., 2019).

111 In addition to satellite sensors, field spectroscopy has also demonstrated great potential
112 and applicability to in-field pasture quality assessments (Pullanagari et al., 2012). Field
113 spectroscopy has also been used to upscale models to satellite data and to simulate the
114 applicability of different satellite spectral resolutions (Fernández-Habas et al., 2021;
115 Lugassi et al., 2019; Mutanga et al., 2015; Ramoelo and Cho, 2018; Sibanda et al.,
116 2015). In this study, we apply this approach to investigate the potential of the CHIME
117 mission to assess the quality of high-diverse Mediterranean permanent grasslands.

118 Machine learning algorithms have a great potential to exploit hyperspectral data and to
119 retrieve grasslands attributes (Verrelst et al., 2015). The number of variables is usually
120 larger than the number of samples and, on the other hand, these data tend to suffer from
121 multicollinearity (Adjorlolo et al., 2013; Rivera-Caicedo et al., 2017). The redundancy
122 and correlation between variables in hyperspectral data lead to the ‘Hughes
123 phenomenon’ where the accuracy of the classification/predictions increases gradually
124 with an increasing number of spectral bands or dimensions to a certain number of bands
125 when it decreases dramatically (Hughes, 1968; Ma et al., 2013). Therefore, the
126 algorithms used have to be efficient in dealing with these issues to avoid the ‘Hughes
127 phenomenon’, also known as ‘curse of dimensionality’ (Rivera-Caicedo et al., 2017;
128 Verrelst et al., 2015). ~~The algorithms used have to be efficient in dealing with these~~
129 ~~issues to avoid the Hughes phenomenon (Verrelst et al., 2015)~~. Two methods are
130 commonly used in remote sensing and chemometrics to analyse hyperspectral data:

131 Partial Least Squares (PLS) regression and Random Forest (RF) regression. These
132 methods have been extensively implemented in remote sensing demonstrating their
133 robustness and reliability (Verrelst et al., 2015). PLS is the state-of-the-art non-
134 parametric method for analysing spectroscopic data, ~~widely used in chemometries~~
135 (Kucheryavskiy, 2018; Wold et al., 2001) and vegetation properties mapping (Biewer,
136 et al., 2009b; Verrelst et al., 2015). RF is an ensemble classification and regression
137 algorithm consisting of an evolution Classification and Regression Trees (CARTs)
138 developed by Breiman (2001) that combines bagging and bootstrapping approaches. It
139 has become popular for remote sensing applications due to its high accuracy, flexibility
140 to be used with complex datasets and few hyperparameters to be set (Belgiu and Drăgu,
141 2016).

142 Previous studies have provided insightful information about the potential of field
143 spectroscopy at different spectral resolutions (Pullanagari et al., 2012). For example,
144 Zhou et al. (2019) demonstrated the feasibility of the Yara N-sensor spectrometer at 10
145 nm spectral resolution to predict the yield and quality of legume and grass mixtures.
146 The recently published research by Pullanagari et al. (2021) provided conclusive results
147 about the prediction of canopy nitrogen concentration in temperate grasslands by a
148 convolutional neural network, PLS and gaussian process regression using field
149 spectroscopy.

150 Although PLS and RF can deal with multicollinearity, feature selection approaches are
151 highly recommended when using hyperspectral data due to the issues mentioned above
152 (Belgiu and Drăgu, 2016). Several studies have demonstrated that predictions using
153 both PLS and RF can benefit from data reduction by feature selection in hyperspectral
154 data (Mansour et al., 2012; Belgiu and Drăgu, 2016; Kawamura et al., 2008). Another
155 important application of this approach is the identification of important bands or the

156 removal of redundant information. PLS and RF can also provide estimates of the bands
157 importance (Belgiu and Drăgu, 2016; Mehmood et al., 2012; Santos-Rufo et al., 2020).
158 This information has relevant implications to: i) inform the use of hyperspectral data ii)
159 optimise the models and data used and iii) inform the design of hyperspectral-based
160 devices (Chan and Paelinckx, 2008; Pullanagari et al., 2012). These approaches of band
161 selection and band importance identification have direct application to the use of the
162 data provided by the forthcoming CHIME mission whose spectrometer is expected to be
163 equipped with 210 bands (Nieke and Rast, 2018). In fact, the Mission Requirements
164 Document by Rast et al. (2019) pointed out that one of the following analyses of the
165 Mission would be to “*confirm the spectral sampling requirements (10 nm at FWHM)*
166 *for the target applications and related products, incl. support to product quality*
167 *specification*”. To the best of our knowledge, the applicability of hyperspectral narrow
168 bands to assess the pasture quality of Mediterranean grasslands has received poor
169 attention. Given the particularities (high heterogeneity and variability) and interest of
170 these ecosystems outlined before, further research focused on this type of grasslands is
171 required to advance in the use of sensing methods in their management and monitoring.
172 In this context, the overall objective of this study was to assess the potential of
173 hyperspectral data CHIME-like at 10nm spectral resolution to estimate pasture quality
174 in Mediterranean permanent grasslands using field spectroscopy. To achieve this goal,
175 we established the following specific objectives:

- 176 i) Evaluate and compare the performance and prediction accuracy of RF and
177 PLS regressions to assess crude protein (CP), neutral detergent fibre (NDF),
178 acid detergent fibre (ADF) and enzyme digestibility of organic matter
179 (EDOM).

- 180 ~~ii)~~—Test the implementation of backward feature elimination techniques (BFE)
181 to optimise the predictive models: and to
182 ~~iii)ii)~~ ii) Identify the most important narrow bands to predict the pasture quality
183 indicators.
184 ~~iv)iii)~~ iii) Interpret the implications of the outcomes for the management and
185 monitoring of Mediterranean permanent grasslands.

186 **2. Material and methods**

187 **2.1. Pasture sampling**

188 Pasture samples were taken in five *Dehesa* farms from the Cordoba province, in the
189 north of Andalusia region (Spain) during the growing season of 2012-2013 (farms 1-4)
190 and 2018-2019 (farm 5) (~~Table 1~~Fig. 1). The pasture sampling conducted in 2012-2013
191 was aimed at studying the grazing effect on pasture quality of natural permanent
192 grasslands of *Dehesas* in a previous study (Fernández et al., 2014). Four sampling
193 quadrats of 0.4 x 0.4 m were randomly set within grazing exclusion plots and four
194 outside of them. This sampling was repeated on five dates; January/February, March,
195 April, May and June which provided 125 samples (Table 1) after removal of those with
196 extremely low pasture biomass for laboratory analysis. Locations of 0.4 x 0.4 m
197 quadrats sampled on previous dates were avoided. In farm 5, pasture samples were
198 collected in May of 2019. Plots of 10x10 m were located in irrigated grasslands (3
199 plots) natural grasslands (3 plots) and improved grasslands with commercial seed
200 mixtures (6 plots). Within each 10 x 10 m plot, four sampling quadrats were randomly
201 set, providing 48 pasture samples. The pasture contained within the quadrats was
202 clipped to ground level, dried in the oven for 48 h at 60°C and ground to pass through a
203 1-mm sieve. In total, 173 samples (Table 1) were analysed at the Laboratory of Animal
204 Nutrition of SERIDA (Villaviciosa, Asturias, Spain) to determine the percentage of

205 crude protein (CP), neutral detergent fibre (NDF), acid detergent fibre (ADF) and
206 enzyme digestibility of organic matter (EDOM). The grasslands sampled consisted of
207 communities mainly dominated by annuals with species such as *Avena* spp., *Astragalus*
208 *pelecinus*, *Bromus* spp., *Diploaxis* spp., *Erodium* spp., *Hordeum* spp., *Lolium* spp.,
209 *Ornithopus compressus*, *Plantago* spp., *Trifolium subterraneum*, *T. cherleri*, *T.*
210 *tomentosum*, *T. glomeratum*, and *Vulpia* spp in natural grasslands, *T. repens* and *Lolium*
211 spp., in the irrigated field and *T. vesiculosum*, *T. michelianum*, *T. resupinatum*, *O.*
212 *compressus* and *L. multiflorum* in improved grasslands from farm 5.

213 **2.2. Canopy reflectance measurement and preprocessing**

214 Before pasture clipping, the reflectance of the pasture contained in the 0.4x0.4 m
215 quadrats was recorded using an ASD FieldSpec Spectroradiometer (ASD Inc, Boulder,
216 Colorado, USA). The measurements were taken under clear sky between 10:00 and
217 15:00. The spectroradiometer records reflectance at a spectral resolution of 1.4 nm
218 within the 350-1000 nm range and 2 nm within the 1000-2500 nm range. The output
219 data is an interpolated reflectance at 1 nm spectral resolution in the whole range of 350-
220 2500 nm. The device is equipped with a fibre optic probe assembled to a pistol grip that
221 is held at 1.20 m height resulting in a 0.22 m² measurement area. Four replicated were
222 recorded per quadrat and averaged to provide a unique representative reflectance
223 measurement of the quadrat. Calibrations on white references were done on a
224 Spectralon panel (Labsphere, NorthSutton, NH) every four samples.

225 The spectra were smoothed applying the Savitzky-Golay (Savitzky and Golay, 1964)
226 filter using a width of filter window of three and second-order of polynomial. Those
227 regions of the spectra displaying noise due to instrumental noise (350-395 nm and 2300-
228 2500 nm), atmospheric noise (1370-1410 nm and 1816-1941 nm) or detector change
229 (1000-1005 nm) were removed. In order to match the spectral specifications of the high-

230 priority candidate mission of the European Space Agency: Copernicus Hyperspectral
231 Imaging Mission for the Environment (CHIME) (Nieke and Rast, 2018), the spectra
232 were resampled to 10 nm spectral resolution using the “*resample2*” function of the
233 CRAN-package “*prospectr*” (Stevens and Ramirez-Lopez, 2015) resulting in 168
234 hyperspectral bands of 10 nm resolution. Spectral outliers were identified by principal
235 component analysis (PCA) (Morellos et al., 2016; Xu et al., 2018). All analyses,
236 preprocessing and modelling were performed in R v. 3.6.1 (R Development Core Team,
237 2019).

238 **2.3. Partial Least Squares**

239 PLS consist of a lineal multivariate regression model that relates a Y matrix of response
240 variables (CP, NDF, ADF or EDOM) with an X matrix of predictor variables (168
241 hyperspectral bands) by decomposing both Y and X in n -orthogonal Latent Variables
242 (LV) to maximise their covariance. PLS models were calibrated by Leave-One-Out
243 cross-validation (LOOCV). The only parameter to be adjusted in PLS, the optimal
244 number of LV, was selected based on the first local minimum of the root mean squared
245 error (RMSE) of the cross-validated predictions. In this study we describe the basic
246 functioning and characteristics of PLS, further information can be found on Geladi and
247 Kowalski (1986), De Jong (1993) and Wold et al. (2001). PLS models were
248 implemented using CRAN-package “*mdatools*” (Kucheryavskiy 2019; Kucheryavskiy
249 2020).

250 **2.4. Random Forest**

251 The RF regression is a machine learning technique that uses the ensemble of a set of
252 Classification and Regression Trees (CARTs) to make predictions (Breiman, 2001). By
253 bagging approach, RF uses two-thirds of the samples (*in-bag* samples) to create n user-

254 defined unpruned and independent trees (*ntrees*). The remaining third of the samples,
255 the so-called *out-of-bag* (OOB) samples, are used to estimate the Mean Squared Error
256 (MSE), known as the OOB error. The OOB error is considered an accurate estimate of
257 the performance of the model (Grimm et al., 2008; Liaw and Wiener, 2002; Mutanga et
258 al., 2012). At each node of the regression trees, instead of choosing the best split among
259 the predictors as in CARTs, RF randomly selects a user-defined number of predictors
260 (*mtry*) (Liaw and Wiener, 2002). The final predicted value is obtained by averaging the
261 predictions of the *ntrees*. The RF algorithm was implemented with CRAN-
262 package “*randomForest*” (Liaw and Wiener, 2002). As explained above, RF has two
263 main hyperparameters, the number of trees to grow (*ntree*) and the number of
264 predictors to select at each node (*mtry*). The default values of “*randomForest*” were
265 used for *ntree* (500 trees) and *mtry* (1/3 of the total number of ~~predictors~~ predictors)
266 since they have shown to be acceptable values and the most common recommendation
267 (Belgiu and Drăgu, 2016; Díaz-Uriarte and Alvarez de Andrés, 2006). To ensure the
268 right choice of these parameters, RMSE was calculated with the default of *mtry*, half of
269 the default, and twice the default as suggested by Liaw and Wiener (2002).

270 **2.5. Band importance and selection by backward feature elimination in PLS** 271 **and RF**

272 The modelling approach followed in this study is schematised in ~~Fig. 1~~ Fig. 2. Band
273 importance in PLS models was measured based on the absolute value of the regression
274 coefficients which is a “*single measure of association between each variable and the*
275 *response*” (Mehmood et al., 2012). Bands with a large absolute magnitude of their
276 associated regression coefficients are expected to have a high impact on the models
277 while small absolute values of regression coefficients indicate that these bands are
278 unimportant or redundant (Garrido Frenich et al., 1995; Kawamura et al., 2008). This

279 technique has shown to be a robust method in variable selection with PLS (Garrido
280 Frenich et al., 1995; Palermo et al., 2009).

281 The most reliable method for variable importance estimation in RF is the so-called
282 “permutation importance”. The rationale of this method consists of randomly permuting
283 a predictor variable X_j (band in this case) and calculating the MSE of the prediction of
284 the OOB set with the remaining predictors. The difference between the MSE when X_j is
285 permuted and the baseline MSE calculated with all predictors (measured as the
286 percentage increase of MSE) is a measure of the variable importance (Strobl et al.,
287 2007). This process is repeated over all predictors. If the predictor X_j is strongly
288 associated with the response, its exclusion from the predictors produces a substantial
289 increase in the MSE.

290 The most important bands for the prediction of the studied pasture quality variables
291 were selected based on backward feature elimination (BFE). The BFE in PLS was
292 carried out by means of the filter method based on removing at each iteration the band
293 with the smallest absolute value of its regression coefficient (Mehmood et al., 2012).
294 After removing the least important band, a LOOCv is performed to select the optimal
295 number of LV and the new regression coefficients recalculated. This process was
296 repeated until only two bands were left. At each step, the coefficient of determination
297 (R^2) and the RMSE of the LOOCv are calculated. A similar method was applied to RF.
298 The least important band (based on the lowest increase in MSE) was removed at each
299 step until only two bands were left (Adam et al., 2014; Díaz-Uriarte and Alvarez de
300 Andrés, 2006; Odindi, 2014). The R^2 and the RMSE of the OOB estimation were also
301 calculated at each step. The selection of the most important set of bands was determined
302 by selecting the model that yielded the highest R^2 and the lowest RMSE of LOOCv and
303 OOB estimates in PLS and RF respectively in the BFE process.

304 To study the effect of the dataset and the stability of the selected bands, the BFE process
305 was repeated n=100 times over 70% of samples selected by bootstrap. The percentage
306 of times that the bands were selected in the 100 repetitions of the BFE was used as an
307 estimate of their stability.

308 **2.6. Assessment of performance and predictive ability of PLS and RF models**

309 Following Kawamura et al. (2008), Mutanga et al. (2004) and Mutanga et al. (2015) a
310 bootstrap approach was applied to test the performance, robustness and predictive
311 ability of the models built with the selected bands by BFE. The original dataset (n=164)
312 was randomly split into 70% for calibration and 30% for independent test. This random
313 split was repeated 100 times. For both, PLS and RF, models were built with the
314 calibration set (70% bootstrapped samples) to predict over the remaining 30%. The R^2 ,
315 RMSE and Ratio of Performance to Deviation (RPD) of the test predictions were
316 recorded. Mean and confidence intervals (CI) (2.5 and 97.5 percentiles) of R^2 , RMSE
317 and RPD were calculated and reported. Following Askari et al. (2015), the performance
318 and predictive ability of the models were assessed considering the thresholds: “poor”
319 accuracy ($RPD < 1.5$ and $R^2 < 0.6$), “moderate” ($1.5 \leq RPD < 2$ and $R^2 \geq 0.60$), “good” (2
320 $\leq RPD < 2.5$ and $R^2 \geq 0.7$) and “excellent” ($RPD \geq 2.5$ and $R^2 \geq 0.8$).

321 **3. Results**

322 **3.1. Statistics of pasture quality variables**

323 Table 2 shows the descriptive statistics of CP, NDF, ADF and EDOM. There was a
324 wide range of data and large variability for all variables. CP had the largest CV with
325 45.4 % while the rest of the variables had a CV close to 19%. These variables also
326 showed high variability across the different dates of sampling (Fig. S1).

3.2. Performance of PLS and RF models with all bands and with bands selected by backward feature elimination

The PCA of the spectral data revealed nine points laying outside the 95% confidence ellipse (Fig. 2 Fig. 3) that were omitted from the dataset used in the analysis.

Overall, the best models were obtained for CP, with R^2 values over 0.70 using all bands and the selected bands with both PLS and RF, having also the smallest RMSE values.

R^2 values for NDF were in the range of 0.52-0.67 and between 0.47-0.59 for EDOM.

ADF was the parameter that showed the worst statistics with R^2 always below 0.50.

PLS outperformed RF in both cases, with all bands and with selected bands for all variables (Table 3). The backward feature elimination improved the performance of the models for all pasture quality variables and for both regression methods, PLS and RF.

The Δ RMSE denotes that the improvement was different depending on the variable and always higher for PLS (Table 3). The greatest improvement (-12.5 Δ RMSE) with selected bands was obtained for CP with PLS regression, which was the model that showed the best performance with $R^2=0.84$ and $RMSE=2.17$ using 21 bands.

Fig. 3 Fig. 4 illustrates the changes of R^2 and RMSE in backward feature elimination in PLS and RF regressions. In both R^2 and RMSE, the changes in PLS models are more evident than in RF, in which the changes are steadier. In the same line, in PLS both parameters R^2 and RMSE show abrupt changes just after the optimal number of bands selected (Fig. 3 Fig. 4). However, in RF after this point, there is a steady interval until the values drop rapidly. RF showed the best results or negligible variations with the default value of $mtry=1/3$ and stabilisation of RMSE before the 500 trees are grown (Fig. S4 Fig. S5 and Fig. S5 Fig. S6) (Belgiu and Drăgu, 2016; Díaz-Uriarte and Alvarez de Andrés, 2006; Liaw and Wiener, 2002).

3.3. Bands selected by backward feature elimination and importance in PLS and RF

The number and proportion of bands selected by backward feature elimination for each pasture quality variable are shown in Table 3. Several differences can be observed between models. PLS tended to select fewer bands than RF in all variables. The variable with a higher proportion of bands selected using backward feature elimination was NDF, for which 15.5% and 48.8% of the bands were selected with PLS and RF respectively (Table 3). Only 7 bands were selected for ADF with PLS while 53 bands were selected using RF. For CP and EDOM, 12.5% and 10.1% were selected with PLS and 32.7% and 20.2% using RF.

The position of these selected bands in the spectral range of 400-2300 nm is illustrated in [Fig. 4](#)[Fig. 5](#). This figure also illustrates the reflectance curve depending on the content of the pasture quality variable. It can be observed how samples with high values of CP and EDOM and low fibre content show higher reflectance values in the Near Infra-Red region (NIR) (800-1300 nm). Again, some differences can be observed between models. Especially concerning the visible region, while in RF the bands located in this region are mostly selected, in PLS these bands are almost absent. The same happened in the region between 800 nm and 900 nm, in which just band 880 was selected for NDF in PLS, whereas in RF several bands were selected in this spectral region.

Bands from the red-edge region (680-750 nm) were commonly selected for all variables using both PLS and RF ([Fig. 4](#)[Fig. 5](#)). Especially the band centered at 700 nm was selected for all models but ADF using PLS. This band also showed high importance and stability in the predictions ([Fig. 64](#)). For example, for the predictions of CP with PLS

375 and RF, this band was the second and the most important band respectively, having also
376 the highest value of stability (Fig. [64](#)).

377 Bands from the NIR (800-1300 nm), especially from 900 nm onwards in PLS, and the
378 shortwave infrared region (SWIR) from 1300-2300 were also intensively selected in
379 most of the variables using both, PLS and RF except for ADF using PLS. Bands 960
380 and 1160 for example were selected with PLS in CP (Fig. [64](#)), and NDF (~~Fig. S1~~[Fig.](#)
381 [S2](#)). Band 1960 was selected in all models for CP and NDF.

382 Fig. [65](#) shows the importance of the bands selected with PLS and RF for CP prediction.
383 The importance for the rest of the variables can be consulted on Supplementary Material
384 (Fig. [S21](#)-[Fig. S43](#)). Overall, bands belonging to sections 1100-1300 nm of the NIR and
385 2100-2300 of the SWIR regions were rated as the most important bands in PLS. For CP,
386 the red-edge region (680-750 nm) was especially important (Fig. [65](#)). In RF models, the
387 most important bands were located at the visible (400-680 nm), especially those
388 belonging to the green and red sections, and red-edge regions.

389 Important differences can be observed in the stability of the variables. In PLS models,
390 some variables highly ranked showed low values of stability. That is the case of band
391 2230, which was the most important band for predicting CP and was selected in only
392 7% of the times that the backward feature elimination was repeated with bootstrapped
393 data (Fig. [64](#)). On the contrary, band 710, with a lower regression coefficient had a
394 stability value of 85%. For CP using PLS, bands 700 and 710 from red-edge and bands
395 1160, 1170 and 1180 from NIR were highly stable (Fig. [4-6](#)). In RF the stability of the
396 top-ranked bands is, overall, more in line with their importance value.

397 **3.4. Predictive ability and robustness of PLS and RF models**

398 CP was the variable with the most accurate and stable predictions with both, PLS and
399 RF regressions (~~Fig. 6~~~~Fig. 7~~). PLS outperformed the predictive ability and robustness
400 of RF for CP and NDF, being the predictive statistics of both methods very similar for
401 ADF and EDOM (~~Fig. 6~~~~Fig. 7~~). The prediction of CP using PLS showed “good”
402 accuracy ($2 \leq \text{RPD} < 2.5$ and $R^2 \geq 0.7$) with a mean R^2 value of 0.82 and a range of 0.68-
403 0.90. The mean $\text{RMSE}=2.23\%$ was low and the mean $\text{RPD}=2.47$ with values ranging
404 from 1.81 to 3.23. These statistics were considerably worse when RF was used. RF
405 models to predict CP produced mean R^2 value of 0.68, mean $\text{RMSE}=3.00\%$ and mean
406 $\text{RPD}=1.82$, indicating “moderate” accuracy ($1.5 \leq \text{RPD} < 2$ and $R^2 \geq 0.60$). For NDF, the
407 PLS models had a “moderate” accuracy with mean values of R^2 and RPD 0.62 and 1.71
408 respectively and mean $\text{RMSE}=6.05\%$. However, the accuracy of NDF models dropped
409 to “poor” when the predictions were made with RF, reporting a mean $R^2=0.47$, mean
410 $\text{RPD}= 1.41$, and mean $\text{RMSE}=7.20\%$. For ADF and EDOM, “poor” accuracy was
411 obtained using both PLS and RF since the RMSE was high and mean values of $R^2 < 0.6$
412 and $\text{RPD} < 1.5$. Only for EDOM predictions with PLS accuracy close to “moderate”
413 was obtained, with mean values of $R^2=0.54$ and $\text{RPD}=1.55$.

414 4. Discussion

415 4.1. Performance of PLS and RF, prediction ability, certainty and backward 416 feature elimination

417 This study compared two machine learning algorithms widely used in remote sensing,
418 PLS and RF. The results showed that PLS outperformed RF in terms of prediction
419 accuracy and certainty of the predictions of CP and NDF (~~Fig. 6~~~~Fig. 7~~). This result
420 differs from several studies reporting higher performance of non-linear algorithms such
421 as Support Vector Machine (SVM), RF or Convolutional neural network (CNN) using
422 hyperspectral data due to their capability to explain complex non-linear relationships in

423 contrast to conventional PLS regression (Pullanagari et al., 2021; Pullanagari et al.,
424 2016; Pullanagari et al., 2018; Ramoelo et al., 2013; Verrelst et al., 2015; Wijesingha et
425 al., 2020; Yao et al., 2015; Zhou et al., 2019). Wijesingha et al. (2020) reported RF
426 outperforming PLS to predict CP and ADF from 194 samples in mountain hay meadows
427 and *Nardus stricta* grasslands using hyperspectral data from UAVs (118 bands of 5 nm
428 spectral resolution, 482–950 nm). However, as Pullanagari et al. (2021) demonstrated
429 using similar data with CNN and PLS, there is a trade off between the number of
430 samples and the performance of the models. In this study, they found that PLS needs a
431 minimum of 200 samples to stabilise the calibration while at least 1500 samples are
432 required for CNN calibration. Little research has been found comparing RF and PLS to
433 predict pasture variables using similar grasslands and comparable hyperspectral canopy
434 reflectance. Further research is needed to explore if the trade off mentioned above
435 between the number of samples and the performance exists comparing RF and PLS
436 regressions.

437 The results reported on the predictive ability of the models indicate that quantitative
438 predictions of “good” accuracy for CP ($2 \leq \text{RPD} < 2.5$ and $R^2 \geq 0.7$) of Mediterranean
439 permanent grasslands can be achieved using data at a spectral resolution of 10nm. The
440 accuracy drops to “moderate” ($1.5 \leq \text{RPD} < 2$ and $R^2 \geq 0.60$) for NDF. Fernández-Habas
441 et al. (2021), also obtained better calibrations for CP and NDF than for ADF and
442 EDOM using Sentinel-2 data to predict pasture quality in Mediterranean permanent
443 grasslands. Therefore, pasture quality maps in Mediterranean grasslands might be based
444 on CP and NDF predictions.

445 The performance of the models was comparable or even better than results reported
446 from previous studies using similar data. For example, Biewer et al. (2009b) obtained
447 $R^2_{\text{CV}} = 0.83$ and $\text{RPD} = 2.4$ to predict CP in pure swards and binary legume-grass

448 mixtures using field spectroscopy of spectral resolution 3 nm and 30 nm in the 350-
449 1000 nm region and 1000-2500 nm region respectively. However, the accuracy obtained
450 for ADF ($R^2_{CV} = 0.75$ and $RPD=2$) was considerably better than in our case. Safari et al.
451 (2016) obtained worse calibrations for CP than Biewer et al. (2009b), despite using
452 higher spectral resolution which was attributed to the heterogeneity of the grasslands
453 and the reduced spectral range up to 1700 nm. The effect of multiple species
454 composition of grasslands in lower regression accuracy was also pointed out by
455 Kawamura et al. (2008) who reported worse mean $R^2=0.62$ but lower mean $RMSE=1.27$
456 to predict CP. Their results for ADF were slightly better than in this study and worse in
457 the case of NDF. Zhou et al. (2019) reported similar statistics of validation ($R^2=0.84$) to
458 predict CP in legume and grass mixtures using the 10nm spectral resolution Yara-N
459 sensor by Support Vector Machine, while worse results were obtained by PLS
460 ($R^2=0.64$). There is still a considerable variation in the accuracy of the results of studies
461 using field spectroscopy to assess pasture quality. The main reasons might be related to
462 variations in sample size and differences in the grasslands assessed (Pullanagari et al.,
463 2012). A key factor that enabled high accuracy to predict CP and NDF in this study is
464 the wide range of the data used to calibrate the models (Table 2), promoted by the
465 heterogeneity and inter-annual variability of Mediterranean grasslands. The growth
466 stage of the grasslands is another factor affecting the canopy reflectance (Zeng and
467 Chen, 2018), and thus the accuracy of the models. In this study, the models have been
468 calibrated using samples from different growth stages and managements to test the
469 accuracy of general models rather than the accuracy of specific models for different
470 growth stages or compositions. Previous studies have investigated the effect of different
471 growth stages and stand mixtures on the estimation of biomass and nutrient contents
472 (Biewer et al., 2009a; Biewer et al., 2009b; Zeng and Chen, 2018; Zhou et al., 2019).

473 Zeng and Chen (2018) showed differences in reflectance of samples from boot stage,
474 peak growth, and dormancy. However, the PLS models showed improved R² from
475 cross-validation and predictions when samples from all three growth stages were
476 combined. Although the reduced number of samples used for the specific growth stages
477 models might have affected the results. They concluded that is feasible to use a model
478 to predict nutrient contents from vegetative to dormancy stages. Biewer et al. (2009a)
479 and Biewer et al. (2009b) reported improved accuracy of predictions of yield and CP by
480 legume-specific calibrations. On the contrary, Zhou et al. (2019) did not find an
481 influence of sites, developmental stage, and species mixtures on the performance of
482 PLS models. Pullanagari et al. (2021) also reported better performance of models using
483 samples from all seasons combined due to a better cover of the variability compared to
484 the season specific models. In agreement with Zhou et al. (2019), we consider that
485 models developed with samples representing different grow stages, managements
486 (grazed or non-grazed) and sites are more generalisable and useful than models
487 calibrated for specific situations. This is especially important in Mediterranean
488 grasslands due to the high heterogeneity promoted by the high species and functional
489 diversity, management, and differing synchrony of growth stages. Thus, specific models
490 might be of limited application in Mediterranean grasslands. As highlighted by Zeng
491 and Chen (2018), the sample diversification of the calibration dataset covering a wide
492 range of situations (phenological stages, sites, management and species composition) is
493 crucial to improve the estimative ability of the models.

494 Compared to results reported using Sentinel-2 by Fernández-Habas et al. (2021) to
495 predict CP and NDF, the accuracy was improved considerably. This demonstrates that
496 future high-priority mission candidate CHIME (Nieke and Rast, 2018), could improve
497 the quality of the predictions and the retrieval of information from grasslands canopy

498 compared to currently operating multispectral sensors (Berger et al., 2020; Obermeier et
499 al., 2019; Rast et al., 2019; Thenkabail et al., 2000). This improvement in the quality of
500 the predictions is especially important in Mediterranean ecosystems due to the higher
501 heterogeneity of the grasslands (Fava et al., 2009), which demands finer spectral
502 resolution to provide accurate information on the grassland's attributes. However, it has
503 to be considered that the spatial resolution of CHIME (20-30 m) will also play a major
504 role in its potential to monitor grasslands ecosystems (Meier et al., 2020). Here we only
505 tested the spectral resolution, further research involving the spatial resolution is required
506 to get a complete picture of the potential of this promising sensor (Casa et al., 2020).

507 These studies should aim at including the spatial resolution of 20-30 m of the CHIME
508 data in the sampling approach, which together with the results provided in this study
509 could additionally contribute to defining the sources of error and uncertainty of models
510 developed with true CHIME data in the future. Lastly, although the simulation of the
511 spectral resolution of satellites from field spectroscopy has been extensively used in
512 previous research (Adjorlolo et al., 2015; Lugassi et al., 2019; Mutanga et al., 2015;
513 Ramoelo and Cho, 2018; Sibanda et al., 2015), the results obtained from this data must
514 be treated as an approximation to the potential of the future satellite, not as the actual
515 performance of it.

516 ~~Fig. 6~~Fig. 7 illustrates the importance of implementing bootstrap approaches to test the
517 performance and predictive ability of the models. Pullanagari et al. (2021) highlighted
518 the relevance of quantifying and reporting the uncertainty of the predictions as well as
519 using an appropriate sample size. The variation of the models' performance statistics
520 associated with the data partition (~~Fig. 6~~Fig. 7) reveals an inherent uncertainty of the
521 dataset. Reporting information of a single model without testing the certainty of the
522 predictions can lead to biased information (Verrelst et al., 2015). In this study, the

523 interpretation of the model performance was associated with its corresponding
524 uncertainty. This is also relevant when implementing this technology in the
525 management and monitoring of grasslands. It is therefore advisable when reporting
526 information of the predictions, supporting it with the corresponding confidence
527 intervals.

528 The improvement achieved by the BFE using both algorithms, PLS and RF, is also
529 consistent with previous literature (Mutanga, 2004; Adam et al., 2014; Díaz-Uriarte and
530 Alvarez de Andrés, 2006; Odindi, 2014; Belgiu and Drăgu, 2016; Kawamura et al.,
531 2017; Santos-Rufo et al., 2020). For example, Kawamura et al. (2008) also reported an
532 important decrease of RMSE in cross-validation for CP, NDF and ADF using PLS and
533 5 nm of spectral resolution of field spectroscopy. The same authors also compared the
534 performance of models using canopy reflectance of the pasture and first derivative
535 reflectance (Kawamura et al., 2008). They found some differences in performance and
536 band selection of models fitted with first derivative reflectance. The spectral
537 preprocessing of the spectra is an interesting topic for future research that, to our
538 knowledge, has not been investigated in deep for pasture quality estimation using field
539 spectroscopy. For example, Dotto et al. (2018) performed a systematic study on 63
540 spectral preprocessing and multivariate prediction models of soil organic carbon by Vis-
541 NIR spectra using a FieldSpec 3 Spectroradiometer (ASD Inc.). These studies could
542 support choices of spectral preprocessing to improve the prediction capability of the
543 models.

544 **4.2.-Importance and stability of bands to predict pasture quality variables**

545 Most of the bands of known absorption features (see Adjorlolo et al. (2013) and
546 Kawamura et al. (2008) for review) or those close to them were selected and highly
547 ranked for the prediction of the corresponding compounds. The results of the bands

548 importance analysis align with results from previous studies highlighting the role of the
549 red-edge region to assess pasture quality due to its relationship to the chlorophyll
550 content of the vegetation ([Adjorlolo et al., 2015](#); Horler, 1983; Kawamura et al., 2008;
551 [Ramoelo et al., 2011](#); Ramoelo and Cho, 2018). Our results showed that this region was
552 commonly selected for all pasture quality variables in both models ([Fig. 4](#)[Fig. 5](#)), being
553 also some bands such as band centred at 700 nm highly stable ([Fig. 5](#)[Fig. 6](#)). In this
554 study, the 700 nm centred band, ranked second and first in PLS and RF models
555 respectively to predict CP. Adjorlolo et al. (2015) also found the 700 nm waveband as
556 the most important according to the PLS' variable importance projection (VIP) to
557 predict nitrogen content in C3 and C4 grass species. They also found a strong
558 relationship between the 720 nm waveband and CP.- This demonstrates the reliability
559 and importance of this region the red-edge region to assess pasture quality. Bands from
560 NIR and SWIR regions were also commonly selected in PLS and RF for CP and NDF
561 (the best-predicted variables). The selection of bands in these regions lies in the well-
562 known absorption features of cellulose, protein, nitrogen, and starch due to C-H, C-N,
563 N-H, and O-H bonds (Carter, 1994; Clark and Lamb, 1991; Curran, 1989; Kawamura et
564 al., 2008; Kokaly, 2001). These results show that a target-oriented selection of bands in
565 these regions can lead to accurate predictions of pasture quality with few bands
566 ([Adjorlolo et al., 2015](#); [Kawamura et al., 2008](#)).

567 The main difference from previous studies is the contrasting selection of bands in the
568 visible region and their importance in RF models compared to PLS models (Fig. 5, Fig.
569 6, and Fig. S2). The visible region is related to the content of the pigment of vegetation
570 (Blackburn, 1998; Ustin et al., 2009). The pigment content is strongly related to the CP
571 and fibre content, and it is subjected to changes of the phenological stages during the
572 growing season. However, as pointed out by Kattenborn et al. (2019), the up-scaling of

573 pigment concentration to the canopy scale is challenging. Although this trend should be
574 carefully interpreted due to the tendency of RF to select a higher number of bands than
575 PLS by backward feature elimination, one possible explanation for that could lie in the
576 fundamental differences between PLS and RF to model the relationship between
577 predictors and the dependent variable. Since PLS is less suitable for deriving strong
578 non-linear relationships than non-linear models (Pullanagari et al., 2021; Verrelst et al.,
579 2015), RF could better capture the relationships between pigments and canopy
580 reflectance in this region of the spectra. This non-linear relationship between reflectance
581 in the visible range and leaf chlorophyll content has been pointed out in previous
582 research (Blackburn, 1998; Gitelson et al., 2003). For example, Qin (2011) attributed an
583 improved pigments content estimation in grape leaves, using hyperspectral data in the
584 400-750 nm spectrum, to a non-linear modelling by SVM.

585 Some of the selected bands showed low stability to the variation of the dataset. This
586 outcome highlights again the importance of testing the uncertainty of the results. The
587 information on the most important bands in these types of studies should be tied to a
588 stability analysis to be more informative. Because of the confounding effect on the
589 reflectance of canopy structure, leaf inclination, plant diversity, plant water content, or
590 different phenological stages (Curran, 1989; Fava et al., 2009; Kattenborn et al., 2019;
591 Pullanagari et al., 2021; Tong and He, 2017; Zhou et al., 2019), the response of the
592 stability of the selected bands in relation to changes in the dataset has important
593 implications to select stable and reliable bands to perform predictions. The stability of
594 band 700 and 710 and 1160-1180 in PLS to predict CP could indicate a strong CP
595 content-reflectance relationship despite the possible cofounding effects mentioned
596 above. However, the bands selected in the region of the spectra from 2000 to 2300 nm
597 reported low stability. This might be caused by the water content of leaves and soil

598 background since Ripple (1986) found the 2080-2350 nm region to be sensitive to both
599 factors. Ramoelo et al. (2011) also highlighted the water effects in the SWIR region for
600 the retrieval of grass nitrogen. In this study, some samples taken in May and June were
601 senescent. The reflectance of senescent grasslands can distinctively show absorption
602 features in the 2006-2196 region of the spectra that otherwise would be masked by the
603 water content in non-senescent grasslands (Mutanga et al., 2004). This can be
604 appreciated in ~~Fig. 4~~Fig. 5 where ~~the~~ reflectance of samples with higher fibre content
605 and lower CP content (senescent conditions), clearly show absorption features in the
606 SWIR region compared to the reflectance of samples with lower fibre content. In RF,
607 the stability was higher, although the considerable number of bands selected might
608 influence that stability measure. Nevertheless, it can be also observed that bands from
609 the SWIR region tend to show lower stability compared to those from the red-edge
610 region. The mix of senescent and non-senescent samples could lead to the lower
611 stability of the SWIR bands in both models. Independent calibration models for
612 different stages could improve the stability of these bands. However, this would reduce
613 the range of the dataset and the generalization of the models since the mix of senescent
614 and non-senescent grasslands is common in Mediterranean grasslands and the transition
615 between both stages is also an important moment to have information about the pasture
616 quality.

617 **4.3. Implication for the management and monitoring of Mediterranean** 618 **permanent grasslands**

619 PLS models calibrated with the selected bands (from the red-edge and NIR regions) by
620 BFE showed good accuracy in the ~~predietio~~predictions, with high $R^2=0.82$ and low
621 mean RMSE=2.23%. These results demonstrate that future sensors at this spectral

622 resolution can provide useful information for the management and monitoring of
623 Mediterranean permanent grasslands.

624 CP content is a crucial attribute of the pasture to inform the management of grasslands
625 and livestock. Having accurate predictions on the content of CP can help the farmers to
626 perform more efficient grazing of Mediterranean grasslands which are subject to high
627 interannual variations of CP. If the predictions can be performed at quantitative level,
628 the utility of the information compared to qualitative predictions increase considerably
629 since it might allow more precise calculation of information such as the carrying
630 capacity of the grasslands or the need and type for supplementary feedstuff for the
631 livestock (Pullanagari et al., 2013; Ramoelo and Cho, 2018; Raab et al., 2020; Starks et
632 al., 2006). If this level of accuracy is achieved with future operational sensors such as
633 CHIME (Nieke and Rast, 2018), this technology might substitute labour manual
634 collection of samples to determine pasture quality (Starks et al., 2004). The difference
635 of precision can be assumed in benefit for spatial predictions acquired on a regular basis
636 in nearly real-time (Pullanagari et al., 2013; Starks et al., 2004). Indeed, pasture quality
637 determination is not frequently performed in farms of Mediterranean permanent
638 grasslands, where the information provided by these determinations might not
639 compensate for the cost of the analysis. Additionally, the delay between manual
640 sampling collection and the reception of the data limits its usefulness since the quality
641 and phenology of Mediterranean grasslands can change rapidly (Pérez-Ramos et al.,
642 2020, Gómez-Giráldez et al. 2020). Therefore, the availability of hyperspectral data can
643 mean a step forward in the adoption of smart farming in Mediterranean grasslands-
644 based farms. However, it has to be considered that a high proportion of Mediterranean
645 grasslands are devoted to traditional small farming (Lowder et al., 2016) for which the

646 implementation of remote sensing technologies might be of limited application and low
647 interest for smallholders.

648 The analysis of the bands importance and stability to predict the pasture quality
649 indicators has important implications to inform the design of devices aimed at
650 optimising the range of the spectra and the spectral resolution used to assess in-field
651 pasture quality. For example, in the case of CP, it has been demonstrated that field
652 spectrometers with a spectral resolution of 10 nm and 19 target-oriented bands can be
653 sufficient to achieve good accuracy of the predictions.

654 Finally, the enhanced accuracy provided by forthcoming CHIME in combination with
655 currently operating services such as Sentinel-2 opens new opportunities to monitor
656 Mediterranean grasslands ecosystems in the context of the next renewal of the Common
657 Agricultural Policy (CAP) (Rast et al., 2019). This technology can be used to assess the
658 compliance of the CAP and Natura 2000 regulations and the conservation status of
659 grasslands ecosystems at the national scale (Griffiths et al., 2020).

660 **5. Conclusion**

661 Concerning the objectives of the study the conclusions are:

- 662 i) Hyperspectral narrow bands from field spectroscopy at 10 nm of spectral
663 resolution CHIME-like show potential to predict CP at good accuracy and
664 NDF at moderate accuracy level in Mediterranean permanent grasslands.
665 ADF and EDOM were predicted with poor accuracy.
- 666 ii) PLS outperformed RF to predict CP and NDF in terms of accuracy and
667 certainty of the predictions.
- 668 iii) BFE can considerably reduce the number of bands used in the predictions
669 while improving the accuracy of the models, especially in PLS regressions.

670 iv) Bands from the red-edge and NIR regions show high importance and
671 stability to assess the best-predicted variables. Bands centred at 700, 710,
672 1160, 1170 and 1180 are highly stable and important to predict CP. The
673 bands belonging to the SWIR region show lower stability.

674 v) These results prove the potential of hyperspectral data and future satellite
675 missions such as CHIME to inform the management and monitoring of
676 Mediterranean permanent grasslands.

677 Further research needs to be carried out to advance towards the applicability of the
678 results here reported to practical farming in Mediterranean permanent grasslands.

679 **Acknowledgements**

680 This study was funded by the following projects:

681 Operational Group GOP2I-HU-16-0018 (Organic beef cattle production based on
682 Pasture in *Dehesa* ecosystem: Production and Commercialisation improvement). Co-
683 funded by the European Union and “Junta de Andalucía” with the European
684 Agricultural Fund for Rural Development (EAFRD) through the “Consejería de
685 Agricultura, Ganadería, Pesca y Desarrollo Sostenible”.

686 European Union's Horizon 2020 research and innovation programme, grant agreement
687 774124, project SUPER-G (Sustainable Permanent Grassland Systems and Policies).

688 PAGOSER-SAT project with code PID2019-107693RR-C22 (MCIU/AEI/FEDER,
689 UE).

690 The study was developed thanks to a PhD fellowship FPU (code FPU18/02876) of the
691 Spanish Ministry of Education awarded to J. Fernández-Habas.

692 The authors would like to thank the three anonymous reviewers for providing insightful
693 suggestions and constructive comments that have helped to significantly improve the
694 manuscript.

695 **References**

696 Adam, E., Mutanga, O., Abdel-Rahman, E. M., Ismail, R., 2014. Estimating standing
697 biomass in papyrus (*Cyperus papyrus* L.) swamp: Exploratory of in situ
698 hyperspectral indices and random forest regression. *Int. J. Remote Sens.* 35, 693–
699 714. <https://doi.org/10.1080/01431161.2013.870676>

700 Adjorlolo, C., Mutanga, O., Cho, M. A., 2015. Predicting C3 and C4 grass nutrient
701 variability using in situ canopy reflectance and partial least squares regression. *Int.*
702 *J. Remote Sens.* 36, 1743-1761. <https://doi.org/10.1080/01431161.2015.1024893>

703 Adjorlolo, C., Mutanga, O., Cho, M. A., Ismail, R., 2013. Spectral resampling based on
704 user-defined inter-band correlation filter: C3 and C4 grass species classification.
705 *Int. J. Appl. Earth Obs. Geoinf.* 21, 535-544.
706 <https://doi.org/10.1016/j.jag.2012.07.011>

707 Askari, M. S., McCarthy, T., Magee, A., Murphy, D. J., 2019. Evaluation of grass
708 quality under different soil management scenarios using remote sensing
709 techniques. *Remote Sens.* 11, 1835. <https://doi.org/10.3390/rs11151835>

710 Askari, M. S., O'Rourke, S. M., Holden, N. M., 2015. Evaluation of soil quality for
711 agricultural production using visible-near-infrared spectroscopy. *Geoderma.* 243–
712 244, 80–91. <https://doi.org/10.1016/j.geoderma.2014.12.012>

713 Belgiu, M., Drăgu, L., 2016. Random forest in remote sensing: A review of applications
714 and future directions. *ISPRS J. Photogramm. Remote Sens.* 114, 24–31.

715 <https://doi.org/10.1016/j.isprsjprs.2016.01.011>

716 Berger, K., Verrelst, J., Féret, J. B., Wang, Z., Woche, M., Strathmann, M., Danner,
717 M., Mauser, W., Hank, T., 2020. Crop nitrogen monitoring: Recent progress and
718 principal developments in the context of imaging spectroscopy missions. Remote
719 Sens. Environ. 242, 111758. <https://doi.org/10.1016/j.rse.2020.111758>

720 Biewer, S., Erasmi, S., Fricke, T., Wachendorf, M., 2009a. Prediction of yield and the
721 contribution of legumes in legume-grass mixtures using field spectrometry.
722 Precision Agric. 10, 128–144. <https://doi.org/10.1007/s11119-008-9078-9>

723 Biewer, S., Fricke, T., Wachendorf, M., 2009**b**. Development of canopy reflectance
724 models to predict forage quality of legume-grass mixtures. Crop Sci. 49, 1917–
725 1926. <https://doi.org/10.2135/cropsci2008.11.0653>

726 Blackburn, G. A., 1998. Quantifying chlorophylls and carotenoids at leaf and canopy
727 scales: An evaluation of some hyperspectral approaches. Remote Sens. Environ.
728 66, 273-285. [https://doi.org/10.1016/S0034-4257\(98\)00059-5](https://doi.org/10.1016/S0034-4257(98)00059-5)

729 Breiman, L., 2001. Random forests. Mach. Learn. 45, 5–32.
730 <https://doi.org/10.1201/9780429469275-8>

731 Carpintero, E., Andreu, A., Gómez-Giráldez, P. J., Blázquez, Á., González-Dugo, M.
732 P., 2020. Remote-Sensing-Based Water Balance for Monitoring of
733 Evapotranspiration and Water Stress of a Mediterranean Oak – Grass Savanna.
734 Water. 12, 1418. <https://doi.org/10.3390/w12051418>

735 Casa, R., Pignatti, S., Pascucci, S., Huang, W., Pepe, M., 2020. Effect of Spatial
736 Resolution on Soil Properties Retrieval from Imaging Spectroscopy: An
737 Assessment of the Hyperspectral Chime Mission Potential. In: IGARSS 2020-2020

738 [IEEE International Geoscience and Remote Sensing Symposium. Waikoloa,](#)
739 [Hawaii, EE.UU., 26 September - 2 October, 2020, pp. 4906–4909.](#)
740 <https://doi.org/10.1109/IGARSS39084.2020.9323268>

741 [Carter, G. A., 1994. Ratios of leaf reflectances in narrow wavebands as indicators of](#)
742 [plant stress. Int. J. Remote Sens. 15, 697-703.](#)

743 Chang, J., Ciais, P., Viovy, N., Soussana, J. F., Klumpp, K., Sultan, B., 2017. Future
744 productivity and phenology changes in European grasslands for different warming
745 levels: implications for grassland management and carbon balance. Carbon
746 Balance Manag. 12, 1–21. <https://doi.org/10.1186/s13021-017-0079-8>

747 Chan, J.C.W., Paelinckx, D., 2008. Evaluation of Random Forest and Adaboost tree-
748 based ensemble classification and spectral band selection for ecotope mapping
749 using airborne hyperspectral imagery. Remote Sens. Environ. 112, 2999-3011.
750 <https://doi.org/10.1016/j.rse.2008.02.011>

751 [Clark, D. H., Lamb, R. C., 1991. Near infrared reflectance spectroscopy: a survey of](#)
752 [wavelength selection to determine dry matter digestibility. J. Dairy Sci. 74, 2200-](#)
753 [2205. https://doi.org/10.3168/jds.S0022-0302\(91\)78393-8](#)

754 Cosentino, S., Porqueddu, C., Copani, V., Patanè, C., Testa, G., Scordia, D., Melis, R.,
755 2014. European grasslands overview: Mediterranean region. In: A. Hopkins, R. P.
756 Collins, M. D. Fraser, V. R. King, D. C. Lloyd, J. M. Moorby., P. R. H. Robson
757 (Eds.), Proceedings of the 25th General Meeting of the European Grassland
758 Federation: The Future of European Grasslands. [Aberystwyth, Wales, UK, 7-11](#)
759 [September 2014, pp. \(41–56\).](#)

760 Curran, P.J., 1989. Remote sensing of foliar chemistry. Remote Sens. Environ. 30,
761 271–278. [https://doi.org/10.1016/0034-4257\(89\)90069-2](https://doi.org/10.1016/0034-4257(89)90069-2)

- 762 De Jong, S., 1993. SIMPLS: an alternative approach to partial least squares regression.
763 Chemom. Intell. Lab. Syst. 18, 251–263. [https://doi.org/10.1016/0169-](https://doi.org/10.1016/0169-7439(93)85002-X)
764 [7439\(93\)85002-X](https://doi.org/10.1016/0169-7439(93)85002-X)
- 765 [Dotto, A. C., Dalmolin, R. S. D., ten Caten, A., Grunwald, S., 2018. A systematic study](#)
766 [on the application of scatter-corrective and spectral-derivative preprocessing for](#)
767 [multivariate prediction of soil organic carbon by Vis-NIR spectra. Geoderma. 314,](#)
768 [262-274. https://doi.org/10.1016/j.geoderma.2017.11.006](#)
- 769 D'Ottavio, P., Francioni, M., Trozzo, L., Sedić, E., Budimir, K., Avanzolini, P.,
770 [Trombetta, M.F., Porqueddu, C., Santilocchi, R., Toderi, M., 2018. Trends and](#)
771 [approaches in the analysis of ecosystem services provided by grazing systems: A](#)
772 [review. Grass Forage Sci., 73, 15–25. https://doi.org/10.1111/gfs.12299](#)
- 773 Díaz-Uriarte, R., Alvarez de Andrés, S., 2006. Gene selection and classification of
774 microarray data using random forest. *BMC Bioinformatics*. 7, 1–14.
775 <https://doi.org/10.1186/1471-2105-7-3>
- 776 Dumont, B., Andueza, D., Niderkorn, V., Lüscher, A., Porqueddu, C., Picon-Cochard,
777 C., 2015. A meta-analysis of climate change effects on forage quality in
778 grasslands: specificities of mountain and mediterranean areas. *Grass Forage Sci.*
779 70, 239–254. <https://doi.org/10.1111/gfs.12169>
- 780 ESA, E. S. A., 2021. Sentinel-2. Retrieved 4 June 2021, from
781 <https://sentinel.esa.int/web/sentinel/missions/sentinel-2>
- 782 Fava, F., Colombo, R., Bocchi, S., Meroni, M., Sitzia, M., Fois, N., Zucca, C., 2009.
783 Identification of hyperspectral vegetation indices for Mediterranean pasture
784 characterization. *Int. J. Appl. Earth Obs. Geoinf.* 11, 233–243.
785 <https://doi.org/10.1016/j.jag.2009.02.003>

786 Fernández-Habas, J., García Moreno, A.M., Hidalgo-Fernández, M.T., Leal-Murillo, J.
787 R., Abellanas Oar, B., Gómez-Giráldez, P. J., González-Dugo, M.P., Fernández-
788 Rebollo, P.et al., 2021. Investigating the potential of Sentinel-2 configuration to
789 predict the quality of Mediterranean permanent grasslands in open woodlands. Sci.
790 Total Environ. 791, 148101. <https://doi.org/10.1016/j.scitotenv.2021.148101>

791 Fernández, P., Carbonero, M.D., García, A., Leal, J.R., Hidalgo, M.T., Vicario, V.,
792 Arrebola, F., González, M.P V., Arrebola, F., González, M.P., 2014. Variación de
793 la proteína bruta y de la digestibilidad de los pastos de dehesa debida a una
794 supresión temporal del pastoreo. In: 53a Reunión Científica de La SEEP. Potes,
795 Cantabria, Spain, 9-12 June 2014.

796 Garrido Frenich, A., Jouan-Rimbaud, D., Massart, D. L., Kuttatharmmakul, S., Galera,
797 M. M., Vidal, J. M., 1995. Wavelength selection method for multicomponent
798 spectrophotometric determinations using partial least squares. *Analyst*, 120, 2787–
799 2792. <https://doi.org/10.1039/AN9952002787>

800 Geladi, P., Kowalski, B. R., 1986. Partial Least-Squares Regression: A tutorial. *Anal.*
801 *Chim. Acta.* ~~186~~, 185, 1–17. [https://doi.org/10.1016/0003-2670\(86\)80028-9](https://doi.org/10.1016/0003-2670(86)80028-9)

802 Giannakopoulos, C., Le Sager, P., Bindi, M., Moriondo, M., Kostopoulou, E., Goodess,
803 C. M., 2009. Climatic changes and associated impacts in the Mediterranean
804 resulting from a 2 °C global warming. *Glob. Planet. Change.* 68, 209–224.
805 <https://doi.org/10.1016/j.gloplacha.2009.06.001>

806 Giorgi, F., Lionello, P., 2008. Climate change projections for the Mediterranean region.
807 *Glob. Planet. Change.* 63, 90–104. <https://doi.org/10.1016/j.gloplacha.2007.09.005>

808 Gitelson, A. A., Gritz, Y., Merzlyak, M. N., 2003. Relationships between leaf
809 chlorophyll content and spectral reflectance and algorithms for non-destructive

810 [chlorophyll assessment in higher plant leaves. J. Plant Physiol. 160, 271-282.](#)
811 [https://doi.org/10.1078/0176-1617-00887](#)

812 Gómez-Giráldez, P. J., Pérez-Palazón, M. J., Polo, M. J., González-Dugo, M. P., 2020.
813 Monitoring grass phenology and hydrological dynamics of an oak-grass savanna
814 ecosystem using sentinel-2 and terrestrial photography. Remote Sens. 12, 1–23.
815 [https://doi.org/10.3390/rs12040600](#)

816 Griffiths, P., Nendel, C., Pickert, J., Hostert, P., 2020. Towards national-scale
817 characterization of grassland use intensity from integrated Sentinel-2 and Landsat
818 time series. Remote Sens. Environ. 238, 111124.
819 [https://doi.org/10.1016/j.rse.2019.03.017](#)

820 Grimm, R., Behrens, T., Märker, M., Elsenbeer, H., 2008. Soil organic carbon
821 concentrations and stocks on Barro Colorado Island - Digital soil mapping using
822 Random Forests analysis. Geoderma. 146, 102–113.
823 [https://doi.org/10.1016/j.geoderma.2008.05.008](#)

824 Horler, D.N.H., Dockray, M., Barber, J., 1983. The red edge of plant leaf reflectance.
825 Int. J. Remote Sens. 4, 273–288. [https://doi.org/10.1080/01431168308948546](#)

826 [Hughes, G., 1968. On the mean accuracy of statistical pattern recognizers. IEEE Trans.](#)
827 [Inf. Theory. 14, 55–63](#)

828 Jouven, M., Lapeyronie, P., Moulin, C. H., Bocquier, F., 2010. Rangeland utilization in
829 Mediterranean farming systems. Animal. 4, 1746–1757.
830 [https://doi.org/10.1017/S1751731110000996](#)

831 [Kattenborn, T., Schiefer, F., Zarco-Tejada, P., Schmidtlein, S., 2019. Advantages of](#)
832 [retrieving pigment content \[\$\mu\text{g}/\text{cm}^2\$ \] versus concentration \[%\] from canopy](#)

833 [reflectance. Remote Sens. Environ. 230, 111195.](#)
834 <https://doi.org/10.1016/j.rse.2019.05.014>

835 Kattenborn, T., Fassnacht, F. E., Schmidlein, S., 2019. Differentiating plant functional
836 types using reflectance: which traits make the difference? Remote. Sens. Ecol.
837 Conserv. 5, 5–19.

838 Kawamura, K., Tsujimoto, Y., Rabenarivo, M., Asai, H., Andriamananjara, A.,
839 Rakotoson, T., 2017. Vis-NIR spectroscopy and PLS regression with waveband
840 selection for estimating the total C and N of paddy soils in Madagascar. Remote
841 Sens. 9, 1081. <https://doi.org/10.3390/rs9101081>

842 Kawamura, K., Watanabe, N., Sakanoue, S., Inoue, Y., 2008. Estimating forage
843 biomass and quality in a mixed sown pasture based on partial least squares
844 regression with waveband selection. Grassl. Sci. 54, 131–145.
845 <https://doi.org/10.1111/j.1744-697x.2008.00116.x>

846 Kokaly, R. F., 2001. Investigating a physical basis for spectroscopic estimates of leaf
847 nitrogen concentration. Remote Sens. Environ., 75, 153–161.
848 [https://doi.org/10.1016/S0034-4257\(00\)00163-2](https://doi.org/10.1016/S0034-4257(00)00163-2)

849 Kucheryavskiy, S., 2018. Analysis of NIR spectroscopic data using decision trees and
850 their ensembles. J. Anal. Test. 2, 274–289. [https://doi.org/10.1007/s41664-018-](https://doi.org/10.1007/s41664-018-0078-0)
851 [0078-0](https://doi.org/10.1007/s41664-018-0078-0)

852 Kucheryavskiy, S., 2019. Package ‘mdatools’.

853 Kucheryavskiy, S., 2020. mdatools – R package for chemometrics. Chemom. Intell.
854 Lab. Syst. 198, 103937. <https://doi.org/10.1016/j.chemolab.2020.103937>

855 Liaw, A., Wiener, M., 2002. Classification and Regression by randomForest. R News,

- 856 2, 18–22.
- 857 Lowder, S. K., Scoet, J., Raney, T., 2016. The Number, Size, and Distribution of Farms,
858 Smallholder Farms, and Family Farms Worldwide. *World Dev.* 87, 16–29.
859 <https://doi.org/10.1016/j.worlddev.2015.10.041>
- 860 Lugassi, R., Zaady, E., Goldshleger, N., Shoshany, M., Chudnovsky, A., 2019. Spatial
861 and temporal monitoring of pasture ecological quality: Sentinel-2-based estimation
862 of crude protein and neutral detergent fiber contents. *Remote Sens.* 11, 799.
863 <https://doi.org/10.3390/rs11070799>
- 864 [Ma, W., Gong, C., Hu, Y., Meng, P., Xu, F., 2013. The Hughes phenomenon in](#)
865 [hyperspectral classification based on the ground spectrum of grasslands in the](#)
866 [region around Qinghai Lake. In: International Symposium on Photoelectronic](#)
867 [Detection and Imaging 2013: Imaging Spectrometer Technologies and](#)
868 [Applications. Beijing, China, 30 August 2013, pp. 89101G.](#)
869 <https://doi.org/10.1117/12.2034457>
- 870 Ma, Z., Liu, H., Mi, Z., Zhang, Z., Wang, Y., Xu, W., [Jiang, L., He, J.S.](#), 2017. Climate
871 warming reduces the temporal stability of plant community biomass production.
872 *Nat. Commun.* 8, 1–7. <https://doi.org/10.1038/ncomms15378>
- 873 Mansour, K., Mutanga, O., Everson, T., Adam, E., 2012. Discriminating indicator grass
874 species for rangeland degradation assessment using hyperspectral data
875 resampled to AISA eagle resolution. *ISPRS J. Photogramm. Remote Sens.* 70,
876 56–65. <https://doi.org/10.1016/j.isprsjprs.2012.03.006>
- 877 Mehmood, T., Liland, K. H., Snipen, L., Sæbø, S., 2012. A review of variable selection
878 methods in Partial Least Squares Regression. *Chemom. Intell. Lab. Syst.* 118, 62–

- 879 69. <https://doi.org/10.1016/j.chemolab.2012.07.010>
- 880 Meier, J., Mauser, W., Hank, T., Bach, H., 2020. Assessments on the impact of high-
881 resolution-sensor pixel sizes for common agricultural policy and smart farming
882 services in European regions. *Comput. Electron. Agric.* 169, 105205.
883 <https://doi.org/10.1016/j.compag.2019.105205>
- 884 Morellos, A., Pantazi, X. E., Moshou, D., Alexandridis, T., Whetton, R., Tziotzios, G.,
885 ~~Wiebenson, J., Bill, R., Mouazen, A.M~~ ~~Wiebenson, J., Bill, R., Mouazen, A.M.~~,
886 2016. Machine learning based prediction of soil total nitrogen, organic carbon and
887 moisture content by using VIS-NIR spectroscopy. *Biosyst. Eng.* 152, 104–116.
888 <https://doi.org/10.1016/j.biosystemseng.2016.04.018>
- 889 Mutanga, O., Skidmore, A. K., Prins, H. H. T., 2004. Predicting in situ pasture quality
890 in the Kruger National Park, South Africa, using continuum-removed absorption
891 features. *Remote Sens. Environ.* 89, 393–408.
892 <https://doi.org/10.1016/j.rse.2003.11.001>
- 893 Mutanga, O., ~~nisimo~~, Adam, E., Adjorlolo, C., Abdel-Rahmanw, E. M., 2015.
894 Evaluating the robustness of models developed from field spectral data in
895 predicting African grass foliar nitrogen concentration using WorldView-2 image as
896 an independent test dataset. *Int. J. Appl. Earth Obs. Geoinf.* 34, 178–187.
897 <https://doi.org/10.1016/j.jag.2014.08.008>
- 898 Mutanga, O., ~~nisimo~~, Adam, E., Cho, M. A., 2012. High density biomass estimation for
899 wetland vegetation using worldview-2 imagery and random forest regression
900 algorithm. *Int. J. Appl. Earth Obs. Geoinf.* 18, 399–406.
901 <https://doi.org/10.1016/j.jag.2012.03.012>
- 902 Myers, N., Mittermeller, R. A., Mittermeller, C. G., Da Fonseca, G. A. B., Kent, J., 2000.

- 903 Biodiversity hotspots for conservation priorities. *Nature*, 403, 853–858.
904 <https://doi.org/10.1038/35002501>
- 905 ~~[Nieke, J., Rast, M., 2018. Towards the Copernicus Hyperspectral Imaging Mission For](#)~~
906 ~~[The Environment \(CHIME\). In: IGARSS 2018–2018 IEEE International](#)~~
907 ~~[Geoscience and Remote Sensing Symposium. Valencia, Spain, 22-27 July 2018,](#)~~
908 ~~[pp.157–159. https://doi.org/10.1109/IGARSS.2018.8518384](#)~~
- 909 ~~[Nieke, J., Rast, M., 2018. Towards the Copernicus Hyperspectral Imaging Mission For](#)~~
910 ~~[The Environment \(CHIME\) European Space Agency / ESTEC, Keplerlaan 1, PO](#)~~
911 ~~[Box 299, 2200 AG Noordwijk ZH, The European Space Agency / ESRIN, via](#)~~
912 ~~[Galileo Galilei, Frascati Rome, Italy. 157–159.](#)~~
- 913 Obermeier, W. A., Lehnert, L. W., Pohl, M. J., Makowski Gianonni, S., Silva, B.,
914 Seibert, R., ~~[Laser, H., Moser, G., Müller, C., Luterbacher, J., Bendix, J.](#)~~, 2019.
915 Grassland ecosystem services in a changing environment: The potential of
916 hyperspectral monitoring. *Remote Sens. Environ.* 232, 111273.
917 <https://doi.org/10.1016/j.rse.2019.111273>
- 918 Odindi, J., Adam, E., Ngubane, Z., Mutanga, O., Slotow, R., 2014. Comparison
919 between WorldView-2 and SPOT-5 images in mapping the bracken fern using the
920 random forest algorithm. *J. Appl. Remote Sens.* 8, 083527.
921 <https://doi.org/10.1117/1.jrs.8.083527>
- 922 Olea, L., San Miguel-Ayanz, A., 2006. The Spanish dehesa. A traditional Mediterranean
923 silvopastoral system linking production and nature conservation. In: J. Lloveras, A.
924 González-Rodríguez, O. Vázquez-Yáñez, J. Piñeiro, O. Santamaría, L. Olea, M. J.
925 Poblacione (Eds.), *Proceedings of the 21st General Meeting of the European*
926 *Grassland Federation: Sustainable Grassland Productivity. Badajoz, Spain, 3-6*

927 [April 2006, \(pp. 3–13\).](#)

928 Palermo, G., Piraino, P., Zucht, H. D., 2009. Performance of PLS regression
929 coefficients in selecting variables for each response of a multivariate PLS for
930 omics-type data. *Adv. Appl. Bioinform. Chem.* 2, 57–70.
931 <https://doi.org/10.2147/aabc.s3619>

932 Pérez-Ramos, I. M., Cambrollé, J., Hidalgo-Galvez, M. D., Matías, L., Montero-
933 Ramírez, A., Santolaya, S., Godoy, Ó., 2020. Phenological responses to climate
934 change in communities of plants species with contrasting functional strategies.
935 *Environ. Exp. Bot.* 170, 103852. <https://doi.org/10.1016/j.envexpbot.2019.103852>

936 Porqueddu, C., Ates, S., Louhaichi, M., Kyriazopoulos, A. P., Moreno, G., del Pozo, A.,
937 [Ovalle, C., Ewing, A.M., Nichols, P.G.H.](#), 2016. Grasslands in ‘Old World’ and
938 ‘New World’ Mediterranean-climate zones: Past trends, current status and future
939 research priorities. *Grass Forage Sci.* 71, 1–35. <https://doi.org/10.1111/gfs.12212>

940 Porqueddu, C., Sanna, F., Franca, A., Casasus, I., Melis, R. A. M., Hadjigeorgiou, I.,
941 2017. The role of grasslands in the less favoured areas of Mediterranean Europe.
942 In: C. Porqueddu, A. Franca, G. Lombardi, G. Molle, G. Peratoner, A. Hopkins
943 (Eds.), *Grassland Science in Europe: Grassland resources for extensive farming
944 systems in marginal lands: major drivers and future scenarios. [Alghero, Sardinia,](#)
945 [Italy](#), 7-10 May 2017, pp. 3–22.*

946 Pullanagari, R. R., Dehghan-Shoar, M., Yule, I. J., Bhatia, N., 2021. Field spectroscopy
947 of canopy nitrogen concentration in temperate grasslands using a convolutional
948 neural network. *Remote Sens. Environ.* 257, 112353 .
949 <https://doi.org/10.1016/j.rse.2021.112353>

950 Pullanagari, R. R., Kereszturi, G., Yule, I. J., 2016. Mapping of macro and micro

951 nutrients of mixed pastures using airborne AisaFENIX hyperspectral imagery.
952 ISPRS J. Photogramm. Remote Sens. 117, 1–10.
953 <https://doi.org/10.1016/j.isprsjprs.2016.03.010>

954 Pullanagari, R. R., Yule, I. J., Tuohy, M. P., Hedley, M. J., Dynes, R. A., King, W. M.,
955 2012. In-field hyperspectral proximal sensing for estimating quality parameters of
956 mixed pasture. *Precis. Agric.* 13, 351–369. [https://doi.org/10.1007/s11119-011-](https://doi.org/10.1007/s11119-011-9251-4)
957 [9251-4](https://doi.org/10.1007/s11119-011-9251-4)

958 Pullanagari, R. R., Kereszturi, G., Yule, I., 2018. Integrating airborne hyperspectral,
959 topographic, and soil data for estimating pasture quality using recursive feature
960 elimination with random forest regression. *Remote Sens.* 10, 1117.
961 <https://doi.org/10.3390/rs10071117>

962 Pullanagari, R. R., King, W. M., Yule, I. J., Thulin, S., Knox, N. M., Ramoelo, A.,
963 2013. Remote Sensing of Pasture Quality. In D. L. Michalk, G. D. Millar, W. B.
964 Badgery., K. M. Broadfoot (Eds.), *Proc. 22nd International Grasslands Congress.*
965 [Sydney, Australia, 15-19 September 2013, pp. 15–19.](#)

966 R Development Core Team 2019. R: A language and environment for statistical
967 computing. R Foundation for Statistical Computing, Vienna, Austria. URL
968 <https://www.R-project.org/>.

969 Raab, C., Riesch, F., Tonn, B., Barrett, B., Meißner, M., Balkenhol, N., Isselstein, J.,
970 2020. Target-oriented habitat and wildlife management: estimating forage quantity
971 and quality of semi-natural grasslands with Sentinel-1 and Sentinel-2 data.
972 *Remote. Sens. Ecol. Conserv.* 6, 381–398. <https://doi.org/10.1002/rse2.149>

973 Ramoelo, A., Skidmore, A. K., Cho, M. A., Mathieu, R., Heitkönig, I. M. A., Dudeni-
974 Tlhone, N., [Schlerf, M., Prins, H.H.T.](#), 2013. Non-linear partial least square

975 regression increases the estimation accuracy of grass nitrogen and phosphorus
976 using in situ hyperspectral and environmental data. ISPRS J. Photogramm. Remote
977 Sens. 82, 27–40. <https://doi.org/10.1016/j.isprsjprs.2013.04.012>

978 Ramoelo, A., Cho, M. A., 2018. Explaining leaf nitrogen distribution in a semi-arid
979 environment predicted on sentinel-2 imagery using a field spectroscopy derived
980 models. Remote Sens., 10, [269](https://doi.org/10.3390/rs10020269). <https://doi.org/10.3390/rs10020269>

981 Ramoelo, A., Cho, M. A., Mathieu, R., Skidmore, A. K., 2014. The potential of
982 Sentinel-2 spectral configuration to assess rangeland quality. In: C. M. U. Neale.,
983 A. Maltese (Eds.), Proc. SPIE 9239, Remote Sensing for Agriculture, Ecosystems,
984 and Hydrology XVI, 92390C. Amsterdam, Netherlands, 11 November 2014, pp.
985 92390C. <https://doi.org/10.1117/12.2067315>

986 Ramoelo, A., Skidmore, A. K., Schlerf, M., Mathieu, R., Heitkönig, I. M. A., 2011.
987 Water-removed spectra increase the retrieval accuracy when estimating savanna
988 grass nitrogen and phosphorus concentrations. ISPRS J. Photogramm. Remote
989 Sens. 66, 408–417. <https://doi.org/10.1016/j.isprsjprs.2011.01.008>

990 Rast, M., Ananasso, C., Bach, H., Ben-Dor, E., Chabrillat, S., Colombo, R., Del Bello,
991 U., Feret, J. B., Giardino, C., Green, R. O., Guanter, L., Marsh, S., Nieke, J., Ong,
992 C. C. H., Rum, G., Schaepman, M. E., Schlerf, M., Skidmore, A. K., Strobl, P.,
993 2019. Copernicus hyperspectral imaging mission for the environment: Mission
994 requirements document. (2.1 ed.) (Mission Requirements Document (MRD); No.
995 ESA-EOPSM-CHIM-MRD-3216). European Space Agency (ESA).
996 http://esamultimedia.esa.int/docs/EarthObservation/Copernicus_CHIME_MRD_v2
997 [.1_Issued20190723.pdf](http://esamultimedia.esa.int/docs/EarthObservation/Copernicus_CHIME_MRD_v2)

998 ~~Rast, M., Ananasso, C., Bach, H., Dor, E., Chabrillat, S., Colombo, R., et al., 2019.~~

999 ~~Copernicus Hyperspectral Imaging Mission for the Environment Mission~~
1000 ~~Requirements Document. In European Space Agency, ESA-EOPSM-CHIM-MRD-~~
1001 ~~3216. Retrieved from www.esa.int~~

1002 REDIAM, 2020. WMS Distribución de las formaciones adehesadas en Andalucía.
1003 http://www.juntadeandalucia.es/medioambiente/mapwms/REDIAM_distribucion_f
1004 [ormaciones_adehesadas?. \(accessed 13 May 2020\).](#)

1005 Ripple, W. J., 1986. Spectral reflectance relationships to leaf water stress. *Photogramm.*
1006 *Eng. Remote. Sensing.* 52, 1669–1675.

1007 Rivera-Caicedo, J. P., Verrelst, J., Muñoz-Marí, J., Camps-Valls, G., Moreno, J., 2017.
1008 *Hyperspectral dimensionality reduction for biophysical variable statistical retrieval.*
1009 *ISPRS J. Photogramm. Remote Sens.* 132, 88-101.
1010 <https://doi.org/10.1016/j.isprsjprs.2017.08.012>

1011 Safari, H., Fricke, T., Wachendorf, M., 2016. Determination of fibre and protein content
1012 in heterogeneous pastures using field spectroscopy and ultrasonic sward height
1013 measurements. *Comput. Electron. Agric.* 123, 256–263.
1014 <https://doi.org/10.1016/j.compag.2016.03.002>

1015 Santos-Rufo, A., Mesas-Carrascosa, F. J., García-Ferrer, A., Meroño-Larriva, J. E.,
1016 2020. Wavelength selection method based on partial least square from
1017 hyperspectral unmanned aerial vehicle orthomosaic of irrigated olive orchards.
1018 *Remote Sens.* 12, 1–20. <https://doi.org/10.3390/rs12203426>

1019 Savitzky, A., Golay, M. J. E., 1964. Smoothing and Differentiation. *Anal. Chem.* 36,
1020 1627–1639.

1021 Sibanda, M., Mutanga, O., Rouget, M., 2015. Examining the potential of Sentinel-2

1022 MSI spectral resolution in quantifying above ground biomass across different
1023 fertilizer treatments. *ISPRS J. Photogramm. Remote Sens.* 110, 55–65.
1024 <https://doi.org/10.1016/j.isprsjprs.2015.10.005>

1025 Sollenberger, L. E., Kohmann, M. M., Dubeux Jr, J. C., Silveira, M. L., 2019. Grassland
1026 management affects delivery of regulating and supporting ecosystem services.
1027 *Crop Sci.* 59, 441–459. <https://doi.org/10.2135/cropsci2018.09.0594>

1028 Starks, P. J., Coleman, S. W., Phillips, W. A., 2004. Determination of forage chemical
1029 composition using remote sensing. *J. Range Manag.* 57, 635–640.
1030 [https://doi.org/10.2111/1551-5028\(2004\)057\[0635:dofccu\]2.0.co;2](https://doi.org/10.2111/1551-5028(2004)057[0635:dofccu]2.0.co;2)

1031 Starks, P. J., Zhao, D., Phillips, W. A., Coleman, S. W., 2006. Development of canopy
1032 reflectance algorithms for real-time prediction of bermudagrass pasture biomass
1033 and nutritive values. *Crop Sci.* 46, 927–934.
1034 <https://doi.org/10.2135/cropsci2005.0258>

1035 Stevens, M. A., Ramirez-Lopez, L. (2015). Package ‘prospectr’.

1036 Strobl, C., Boulesteix, A. L., Zeileis, A., Hothorn, T., 2007. Bias in random forest
1037 variable importance measures: Illustrations, sources and a solution. *BMC*
1038 *Bioinformatics*. 8, 1–21. <https://doi.org/10.1186/1471-2105-8-25>

1039 Thenkabail, P. S., Smith, R. B., De Pauw, E., 2000. Hyperspectral vegetation indices
1040 and their relationships with agricultural crop characteristics. *Remote Sens.*
1041 *Environ.* 71, 158-182. [https://doi.org/10.1016/S0034-4257\(99\)00067-X](https://doi.org/10.1016/S0034-4257(99)00067-X)

1042 Tong, A., He, Y., 2017. Estimating and mapping chlorophyll content for a
1043 heterogeneous grassland: Comparing prediction power of a suite of vegetation
1044 indices across scales between years. *ISPRS J. Photogramm. Remote Sens.* 126,

1045 146–167. <https://doi.org/10.1016/j.isprsjprs.2017.02.010>

1046 [Ustin, S. L., Gitelson, A. A., Jacquemoud, S., Schaepman, M., Asner, G. P., Gamon, J.](#)
1047 [A., Zarco-Tejada, P., 2009. Retrieval of foliar information about plant pigment](#)
1048 [systems from high resolution spectroscopy. Remote Sens. Environ. 113, 67-77.](#)
1049 <https://doi.org/10.1016/j.rse.2008.10.019>

1050 Verrelst, J., Camps-Valls, G., Muñoz-Marí, J., Rivera, J. P., Veroustraete, F., Clevers, J.
1051 G. P. W., Moreno, J., 2015. Optical remote sensing and the retrieval of terrestrial
1052 vegetation bio-geophysical properties - A review. ISPRS J. Photogramm. Remote
1053 Sens. 108, 273–290. <https://doi.org/10.1016/j.isprsjprs.2015.05.005>

1054 Wijesingha, J., Astor, T., Schulze-Brüninghoff, D., Wengert, M., Wachendorf, M.,
1055 2020. Predicting Forage Quality of Grasslands Using UAV-Borne Imaging
1056 Spectroscopy. Remote Sens. 12, 126. <https://doi.org/10.3390/rs12010126>

1057 Wold, S., Sjöström, M., Eriksson, L., 2001. PLS-regression: A basic tool of
1058 chemometrics. Chemom. Intell. Lab. Syst. 58, 109–130.
1059 [https://doi.org/10.1016/S0169-7439\(01\)00155-1](https://doi.org/10.1016/S0169-7439(01)00155-1)

1060 Xu, S., Zhao, Y., Wang, M., Shi, X., 2018. Comparison of multivariate methods for
1061 estimating selected soil properties from intact soil cores of paddy fields by Vis–
1062 NIR spectroscopy. Geoderma. 310, 29–43.
1063 <https://doi.org/10.1016/j.geoderma.2017.09.013>

1064 Yao, X., Huang, Y., Shang, G., Zhou, C., Cheng, T., Tian, Y., [Cao, W., Zhu, Y.](#), 2015.
1065 Evaluation of six algorithms to monitor wheat leaf nitrogen concentration. Remote
1066 Sens. 7, 14939–14966. <https://doi.org/10.3390/rs71114939>

1067 [Zeng, L., Chen, C., 2018. Using remote sensing to estimate forage biomass and nutrient](#)

1068 [contents at different growth stages. Biomass bioenergy. 115, 74–81.](#)
1069 <https://doi.org/10.1016/j.biombioe.2018.04.016>
1070 Zhou, Z., Morel, J., Parsons, D., Kucheryavskiy, S. V., Gustavsson, A. M., 2019.
1071 Estimation of yield and quality of legume and grass mixtures using partial least
1072 squares and support vector machine analysis of spectral data. Comput. Electron.
1073 Agric. 162, 246–253. <https://doi.org/10.1016/j.compag.2019.03.038>

Table 1. Grassland type, number of samples and date of sampling of the farms used in the study.

Farm	Coordinates*	Grassland type	Sampling date	Number of samples
1	x= 315534.34 y= 4263109.14	Permanent natural grasslands	2012/2013 January/ February March April May June	28
2	x= 350946.02 y= 4244905.06	Permanent natural grasslands	2012/2013 January/ February March April May June	33
3	x= 352598.98 y= 4235836.66	Permanent natural grasslands	2012/2013 January/ February March April May June	33
4	x= 387377.62 y= 4230454.12	Permanent natural grasslands	2012/2013 January/ February March April May June	31
		Permanent natural grasslands		12
5	x= 331065.33 y= 4197542.60	Reseeded grasslands	2018/2019 May	24
		Irrigated grasslands		12
Total samples				173

*Projected coordinate system: ETRS 1989 UTM Zone 30N

Table 2. Descriptive statistics of the pasture quality variables used to fit the models.

Pasture variables (% of DM)	Minimum	Mean	Maximum	Range	SD	CV
CP	3.7	11.9	27.7	24.0	5.4	45.4
NDF	24.9	52.0	71.3	46.5	10.1	19.4
ADF	15.7	31.8	44.8	29.1	6.2	19.4
EDOM	38.5	58.4	86.2	47.8	10.8	18.4

CP: crude protein; NDF: neutral detergent fibre; ADF: acid detergent fibre; EDOM: enzyme digestibility of organic matter; SD: standard deviation; CV: coefficient of variation.

Table 3. Performance of PLS and RF models with all bands and with selected bands. Coefficient of determination R^2 and root mean square error (RMSE) correspond to leave-one-out and out-of-bag estimations for PLS and RF respectively.

Pasture variables (% of DM)	Model	All bands			Selected bands					
		NLV	R^2	RMSE	NL V	R^2	RMSE	NBS	%BS	Δ RMSE
CP	PLS	11	0.79	2.48	11	0.84	2.17	21	12.5	-12.5
	RF	-	0.70	2.95	-	0.71	2.89	55	32.7	-2.0
NDF	PLS	11	0.60	6.34	10	0.67	5.77	26	15.5	-9.0
	RF	-	0.52	6.98	-	0.53	6.86	82	48.8	-1.7
ADF	PLS	3	0.40	4.74	6	0.46	4.52	7	4.2	-4.6
	RF	-	0.42	4.68	-	0.45	4.55	53	31.5	-2.8
EDOM	PLS	9	0.53	7.35	6	0.59	6.89	17	10.1	-6.3
	RF	-	0.47	7.83	-	0.51	7.52	34	20.2	-4.0

N=164; NBS: number of bands selected by backward feature elimination; %BS: percentage of bands selected from the original dataset (n=168); Δ RMSE: decrease in root mean squared error from model with all bands to models with selected bands. CP: crude protein; NDF: neutral detergent fibre; ADF: acid detergent fibre; EDOM: enzyme digestibility of organic matter

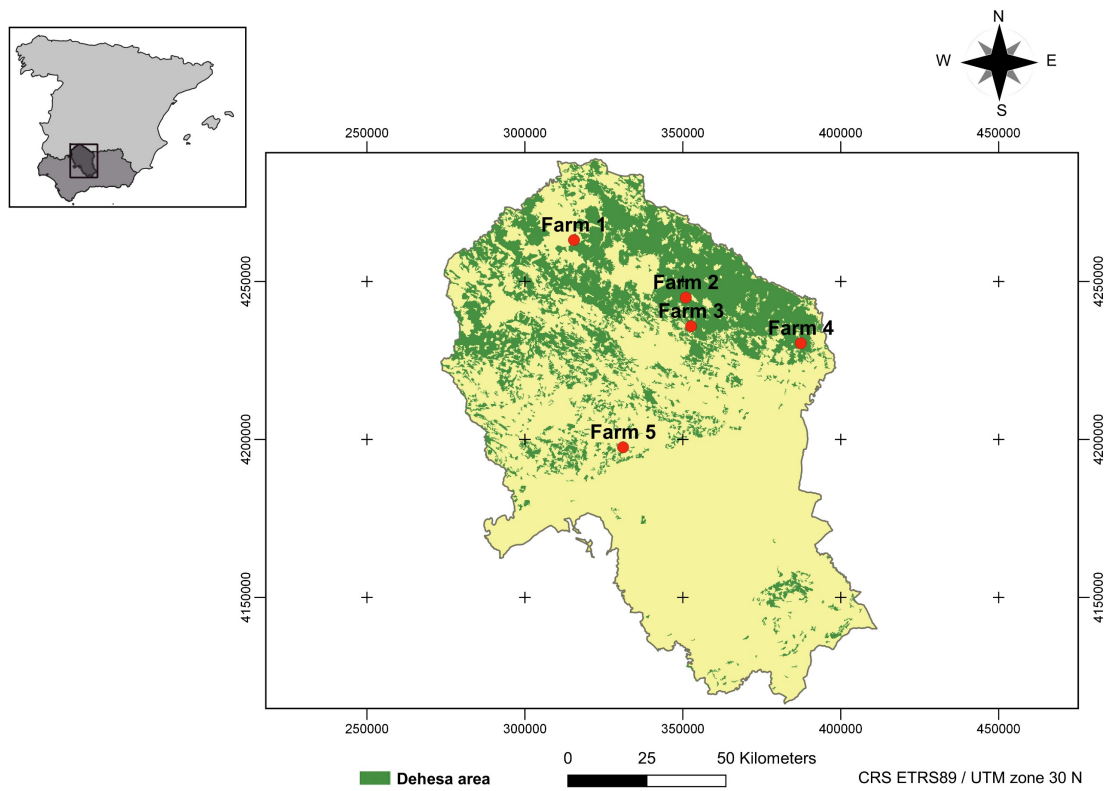


Fig. 1. Location of farms where the grasslands samplings were performed. Farms are located within the *Dehesa* area of Cordoba province, in the north of Andalusia region (Spain). *Dehesa* area layer, coloured in green, is provided by the WMS of the *Dehesa* systems distribution in Andalusia (REDIAM, 2020).

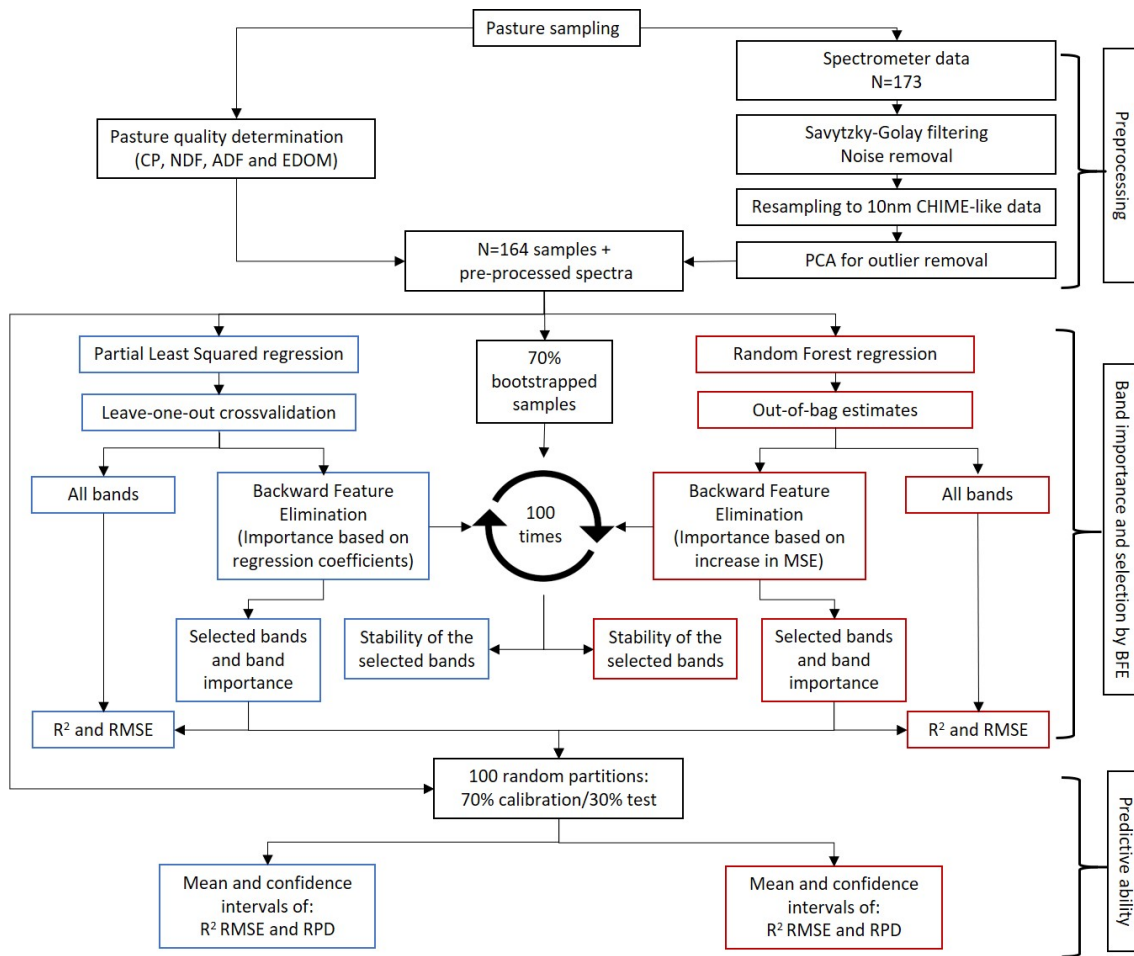


Fig. 2. Modelling approach of the study.

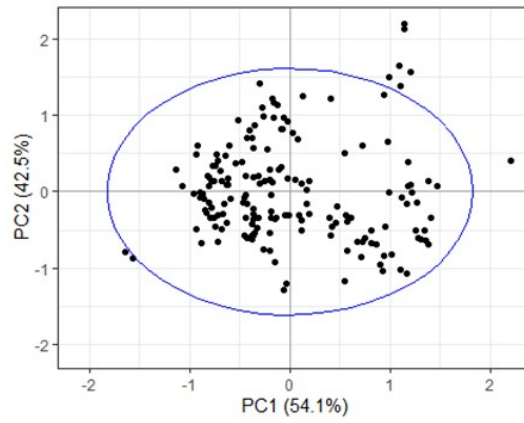


Fig. 3. Detection of outliers after principal component analysis (PCA) of the pasture samples (n=173). Blue line represents 95% confidence ellipse.

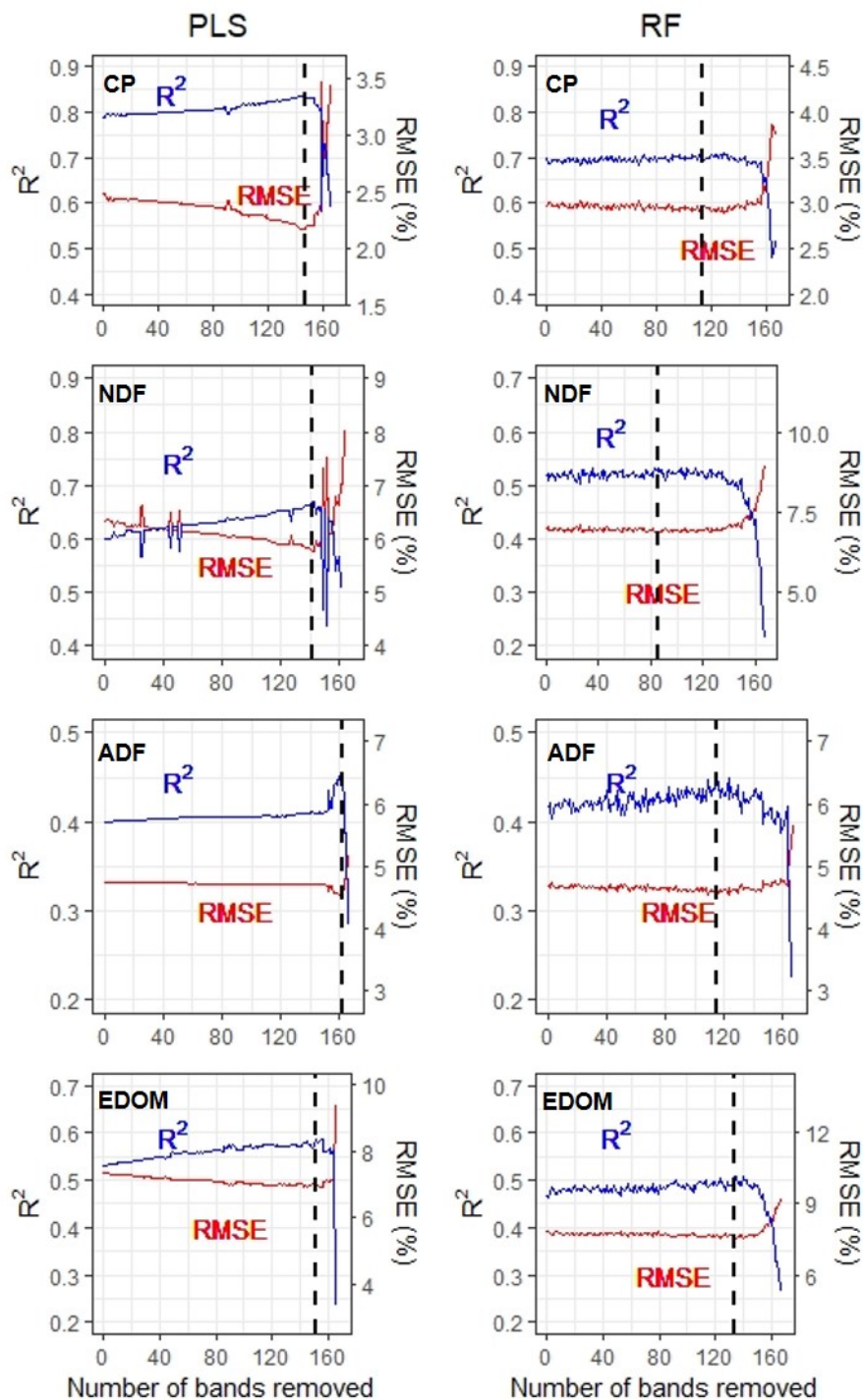


Fig. 4. Changes of R^2 and RMSE in backward feature elimination of redundant bands using PLS (leave-one-out estimations) and RF (out-of-bag estimations) regressions for crude protein (CP), neutral detergent fibre (NDF), acid detergent fibre (ADF), and enzyme digestibility of organic matter (EDOM) ($n=164$). Dashed lines indicate the minimum RMSE value and maximum R^2 at which the optimal number of bands is reached.

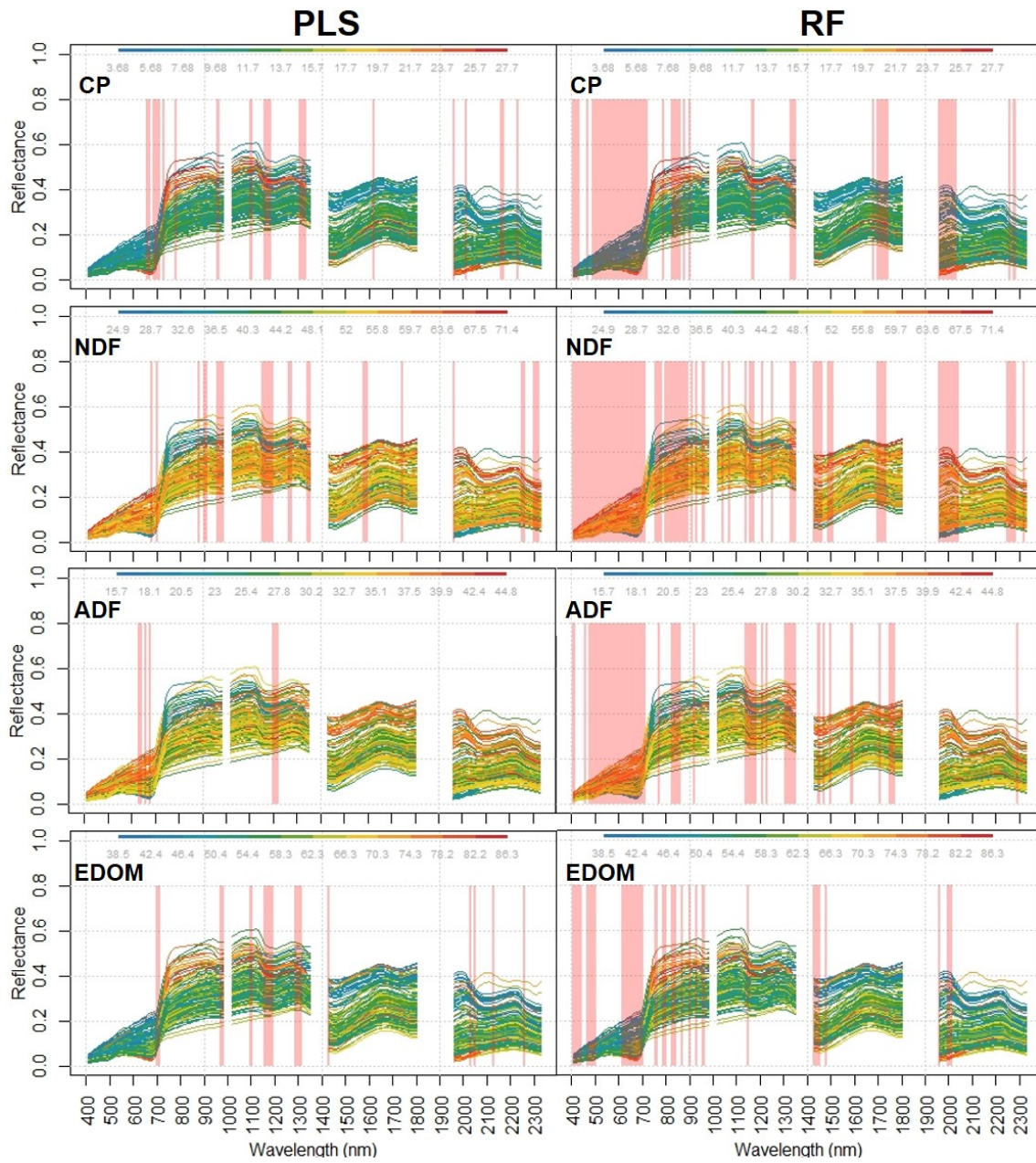


Fig. 5. Canopy reflectance of the pasture samples ($n=164$) coloured by the content of the respective pasture quality variable: crude protein (CP); neutral detergent fibre (NDF); acid detergent fibre (ADF); and enzyme digestibility of organic matter (EDOM). Vertical red lines indicate the selected bands by backward stepwise feature elimination using PLS (left) and RF (right).

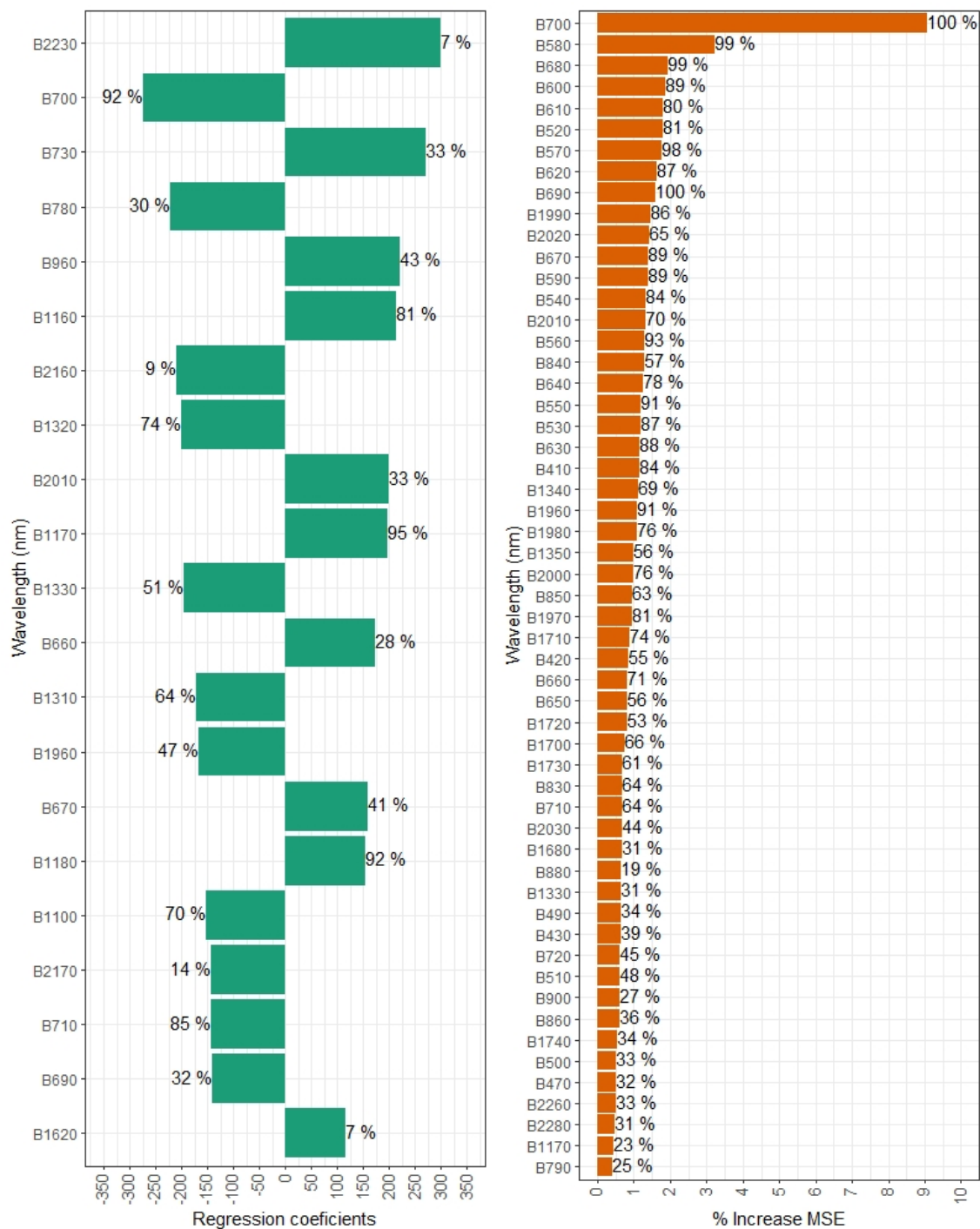


Fig. 6. Importance and stability of selected bands for crude protein (CP) by backward stepwise feature elimination with PLS (21 bands) and RF (55 bands). Importance is measured in absolute value of the regression coefficients of selected bands in PLs and in % increase of mean squared error (MSE) in RF. Stability is indicated as % times the bands were selected in 100 repetitions of the backward feature elimination with using 70% of the samples each time selected by bootstrap with replacement.

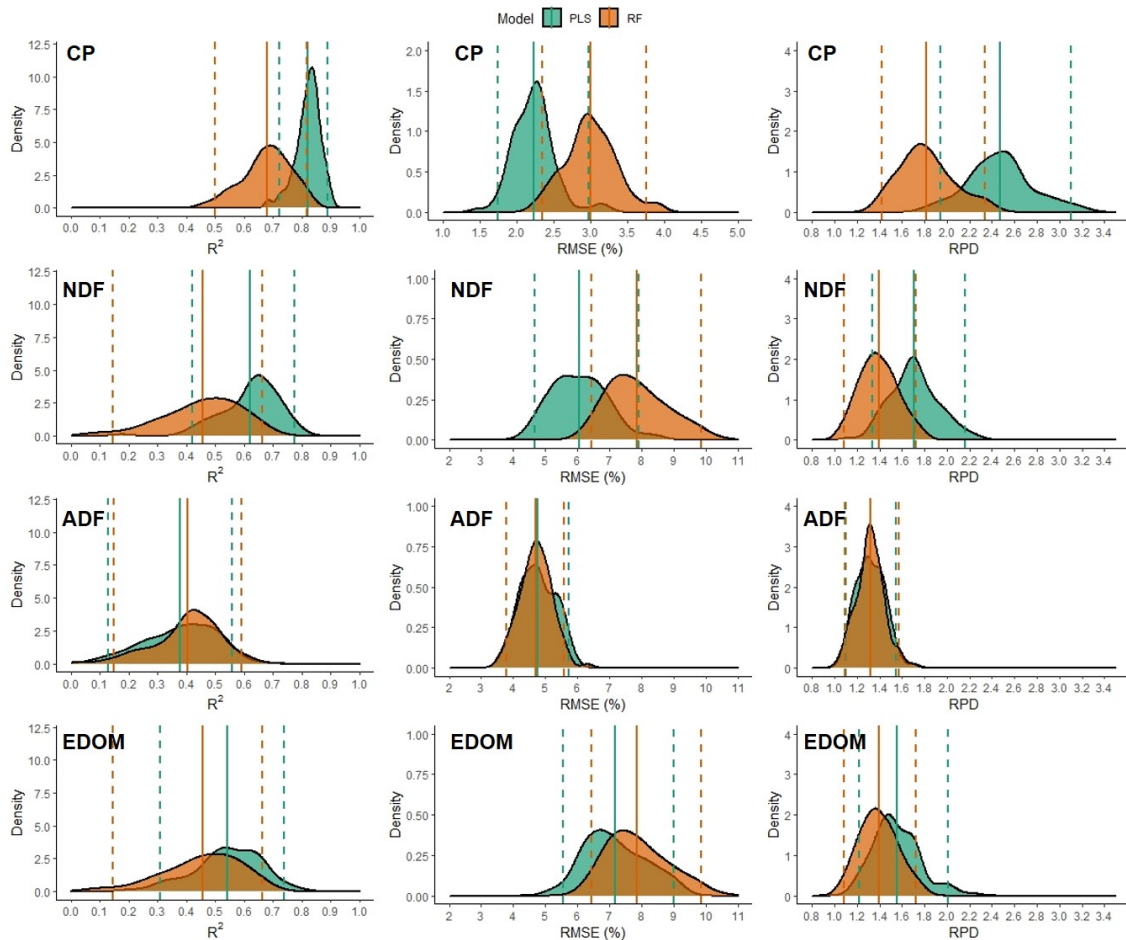


Fig. 7. Density distribution of values of R^2 , root mean square error (RMSE %) and ratio of predicted deviation (RPD) from predictions over 30% of bootstrapped samples using PLS and RF models. Calculated from $n=100$ random partitions of the dataset ($n=164$) into 70% for calibration and 30% for test with replacement. The predicted parameters are; crude protein (CP); neutral detergent fibre (NDF); acid detergent fibre (ADF); and enzyme digestibility of organic matter (EDOM). Solid lines show the mean and dashed lines show the confidence intervals (2.5 and 97.5 percentiles).

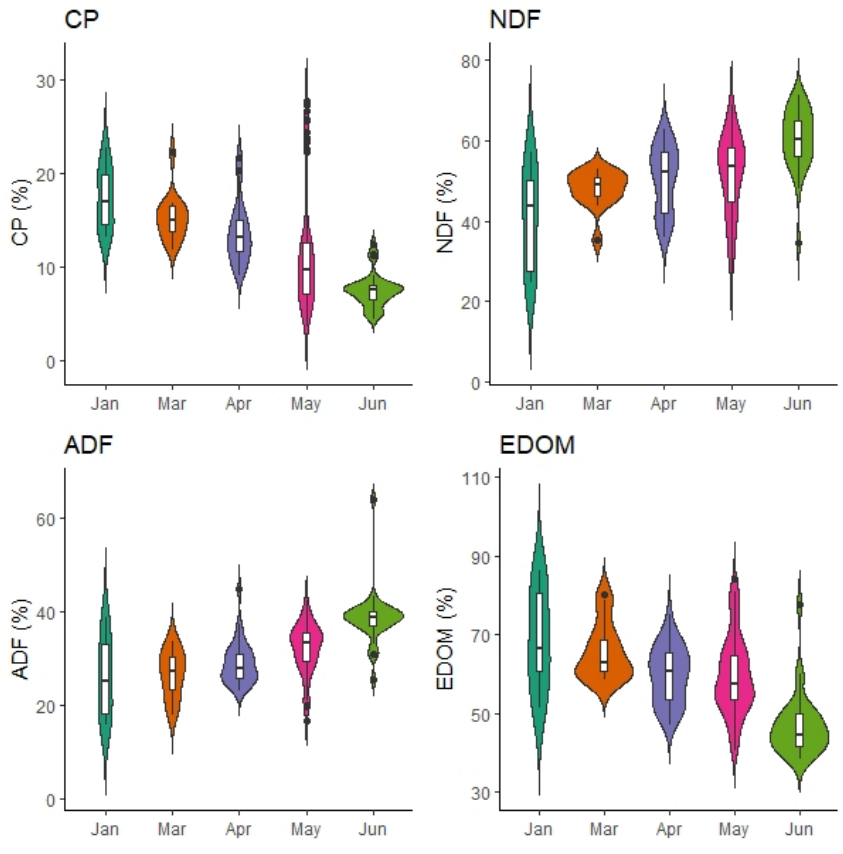
1 **Estimating pasture quality of Mediterranean grasslands using hyperspectral**
2 **narrow bands from field spectroscopy by Random Forest and PLS regressions**

3 Jesús Fernández-Habas^a, Mónica Carriere Cañada^a, Alma María García Moreno^a, José
4 Ramón Leal-Murillo^a, María P González-Dugo^b, Begoña Abellanas Oar^a, Pedro J.
5 Gómez-Giráldez^b, Pilar Fernández-Rebollo^a

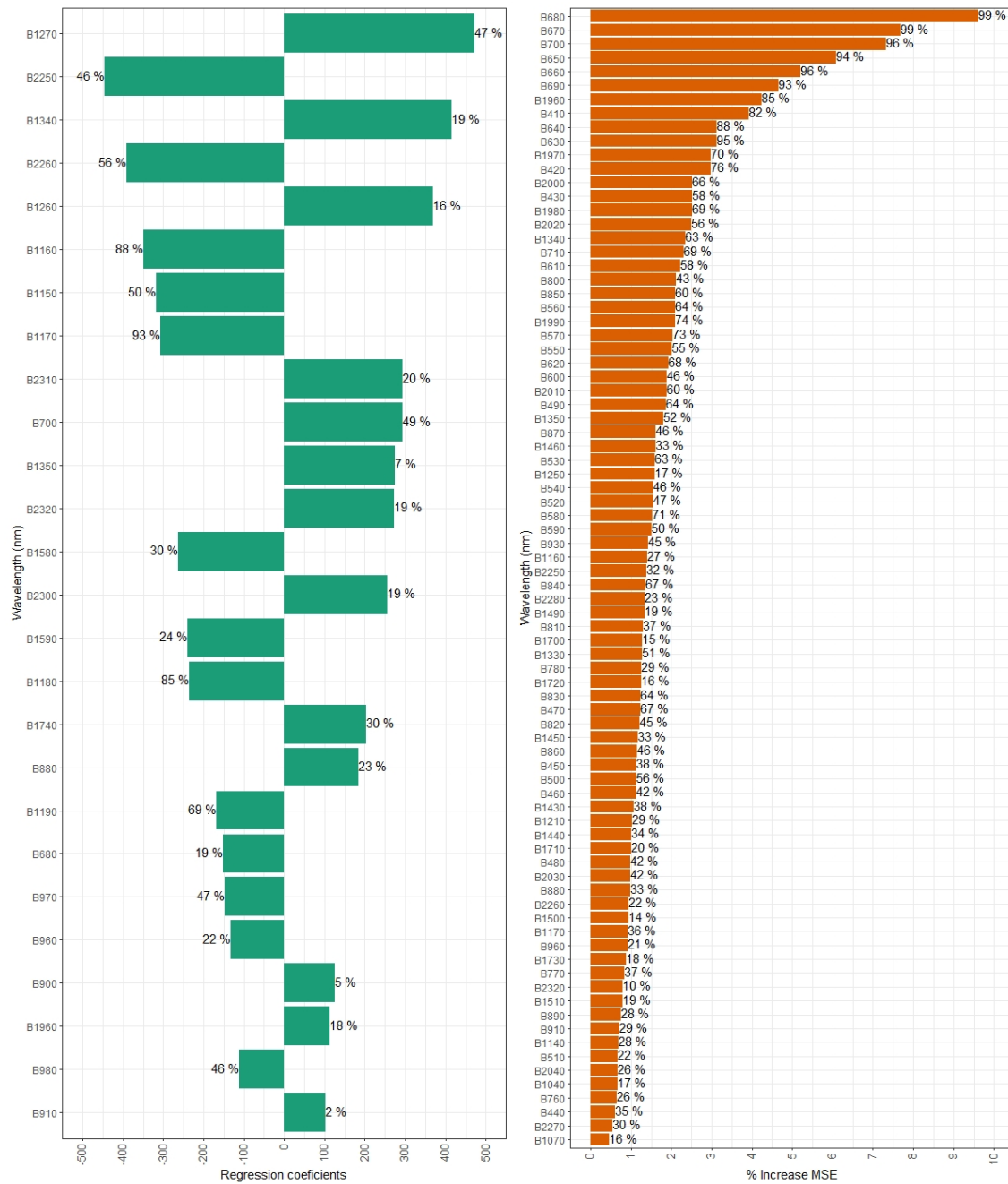
6
7 ^a Department of Forest Engineering, ETSIAM, University of Cordoba, Ctra. Madrid,
8 Km 396. 14071 Córdoba, Spain.

9 ^bIFAPA, Institute of Agricultural and Fisheries Research and Training of Andalusia,
10 Avd. Menéndez Pidal s/n, 14071 Cordoba, Spain.

11
12 **Supplementary material**



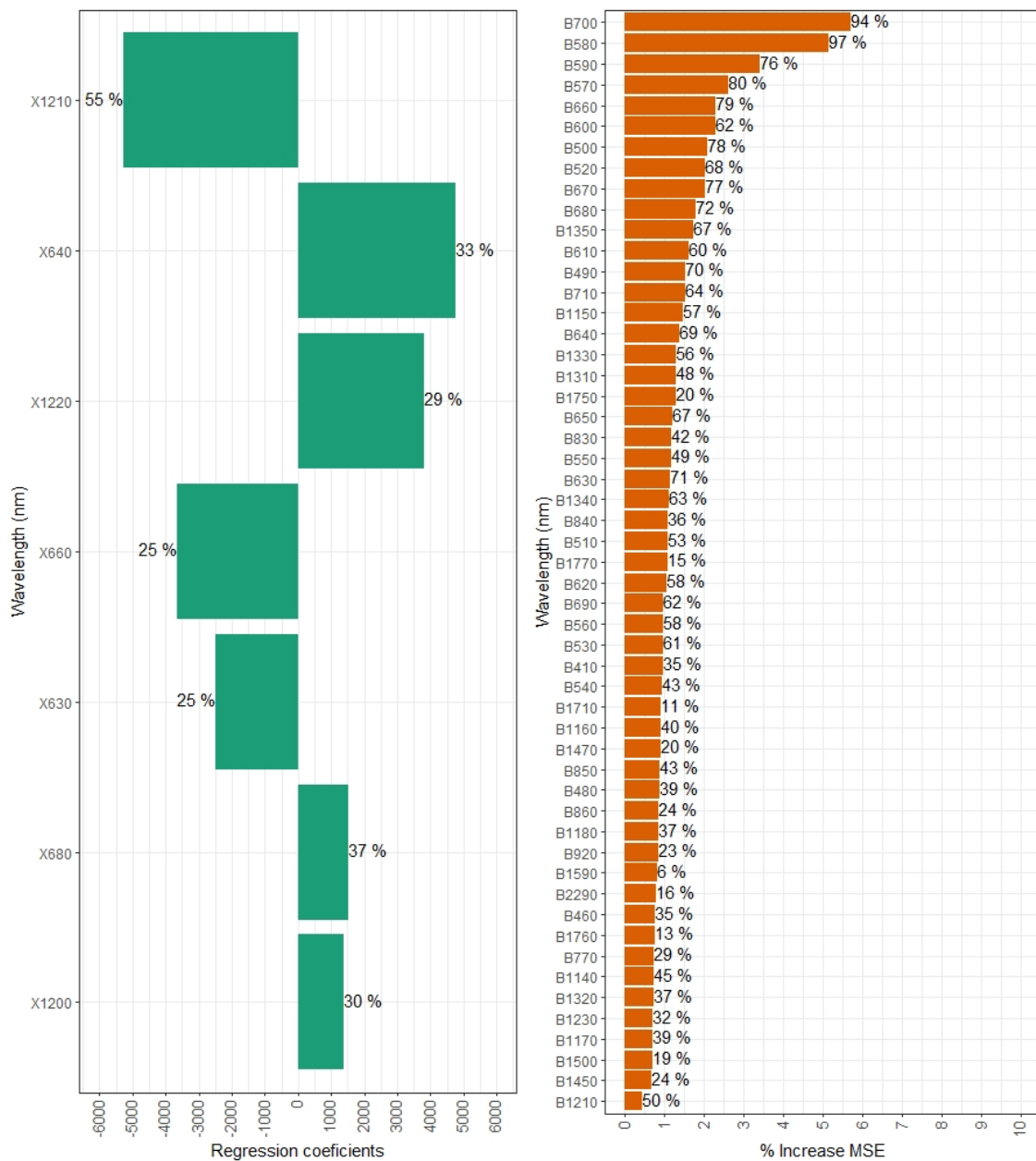
29 **Fig. S1.** Variation of pasture quality variables used to fit the models (N=164) by month.
30 Black centre line, median; box, interquartile range; box limits, lower and upper
31 quartiles; whiskers, 1.5× interquartile range; points, outliers. Coloured area indicates the
32 sample distribution. *May includes samples from 2013 and 2019. CP: crude protein;
33 NDF: neutral detergent fibre; ADF: acid detergent fibre; and EDOM: enzyme
34 digestibility of organic matter.



35

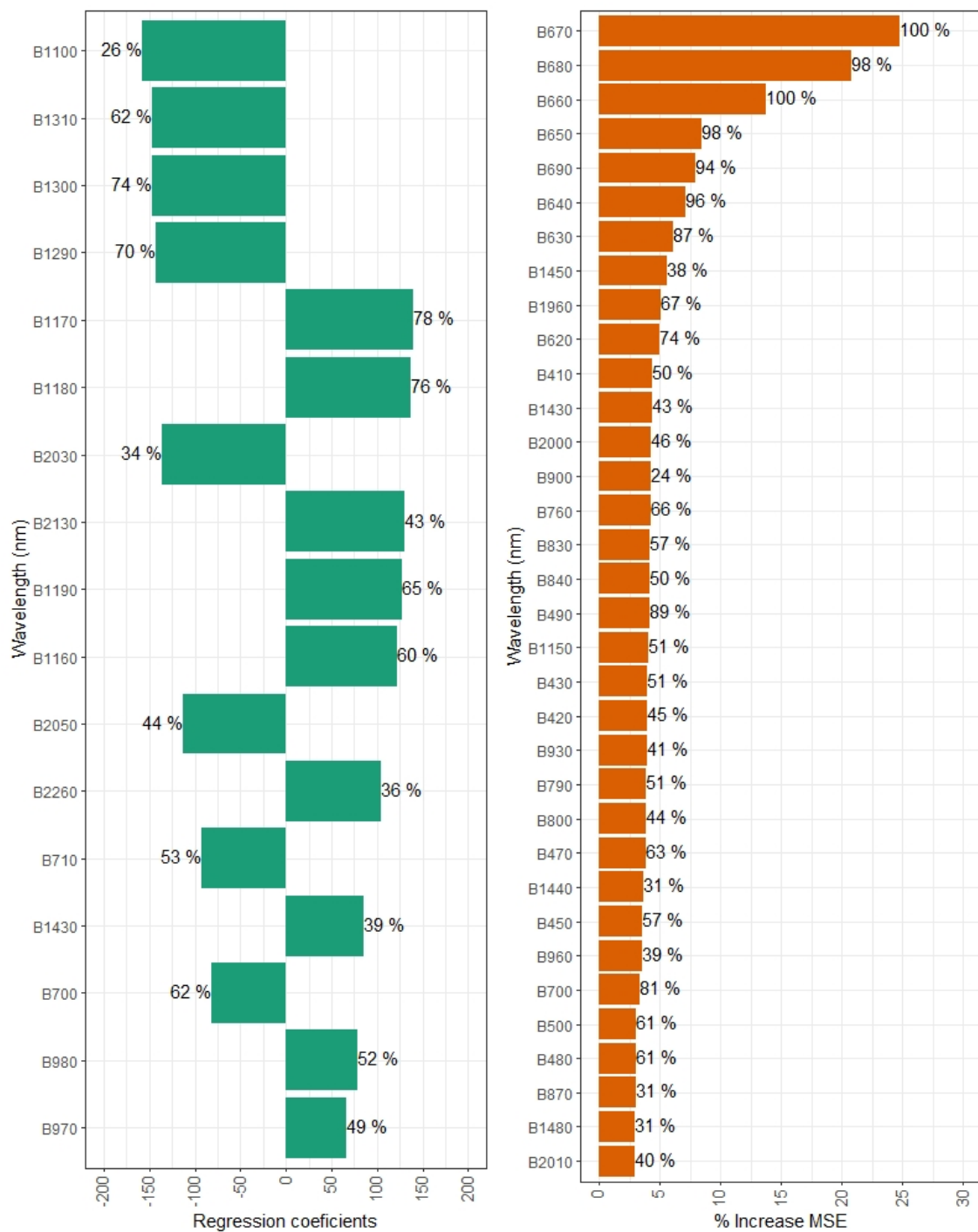
36 **Fig. S2.** Importance and stability of selected bands for neutral detergent fibre (NDF) by
 37 backward stepwise feature elimination with PLS (21 bands) and RF (55 bands).
 38 Importance is measured in the absolute value of the regression coefficients of selected
 39 bands in PLs and in % increase of mean squared error (MSE) in RF. Stability is
 40 indicated as % of times the bands were selected in 100 repetitions of the backward
 41 feature elimination with using 70% of the samples each time selected by bootstrap with
 42 replacement.

43



44

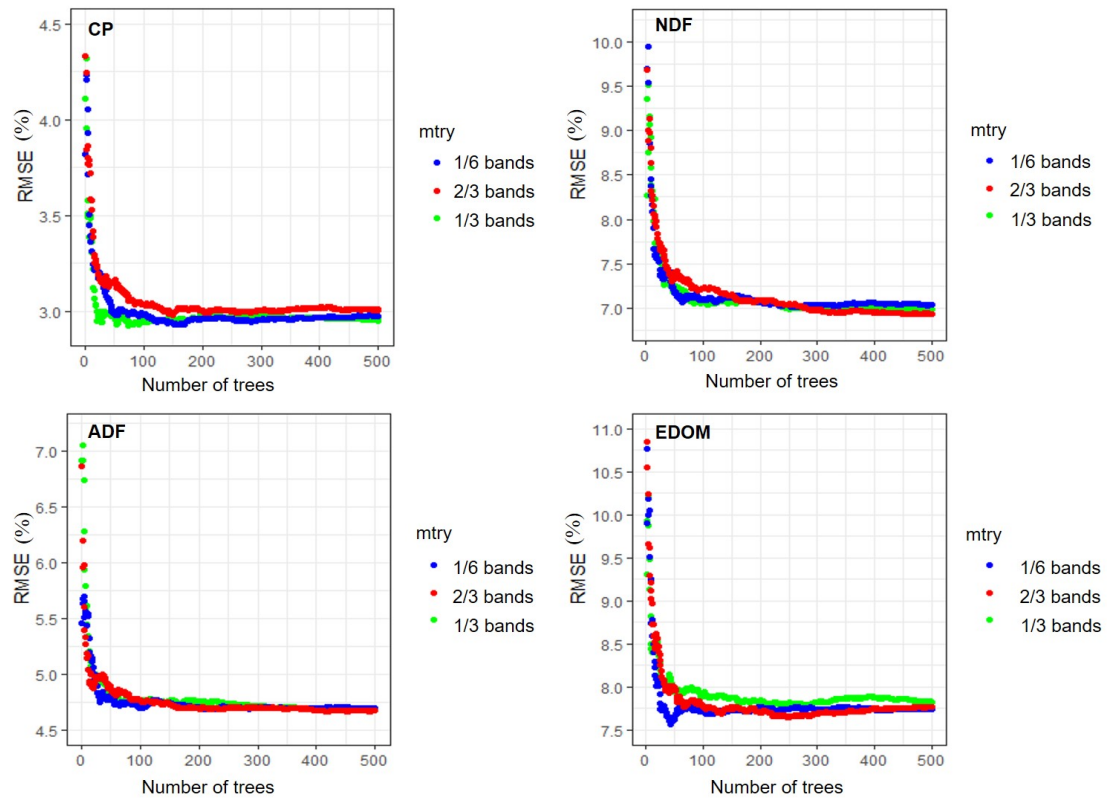
45 **Fig. S3.** Importance and stability of selected bands for acid detergent fibre (ADF) by
 46 backward stepwise feature elimination with PLS (21 bands) and RF (55 bands).
 47 Importance is measured in the absolute value of the regression coefficients of selected
 48 bands in PLs and in % increase of mean squared error (MSE) in RF. Stability is
 49 indicated as % of times the bands were selected in 100 repetitions of the backward
 50 feature elimination with using 70% of the samples each time selected by bootstrap with
 51 replacement.



52

53 **Fig. S4.** Importance and stability of selected bands for enzyme digestibility of organic
 54 matter (EDOM) by backward stepwise feature elimination with PLS (21 bands) and RF
 55 (55 bands). Importance is measured in the absolute value of the regression coefficients
 56 of selected bands in PLs and in % increase of mean squared error (MSE) in RF.
 57 Stability is indicated as % of times the bands were selected in 100 repetitions of the
 58 backward feature elimination with using 70% of the samples each time selected by
 59 bootstrap with replacement.

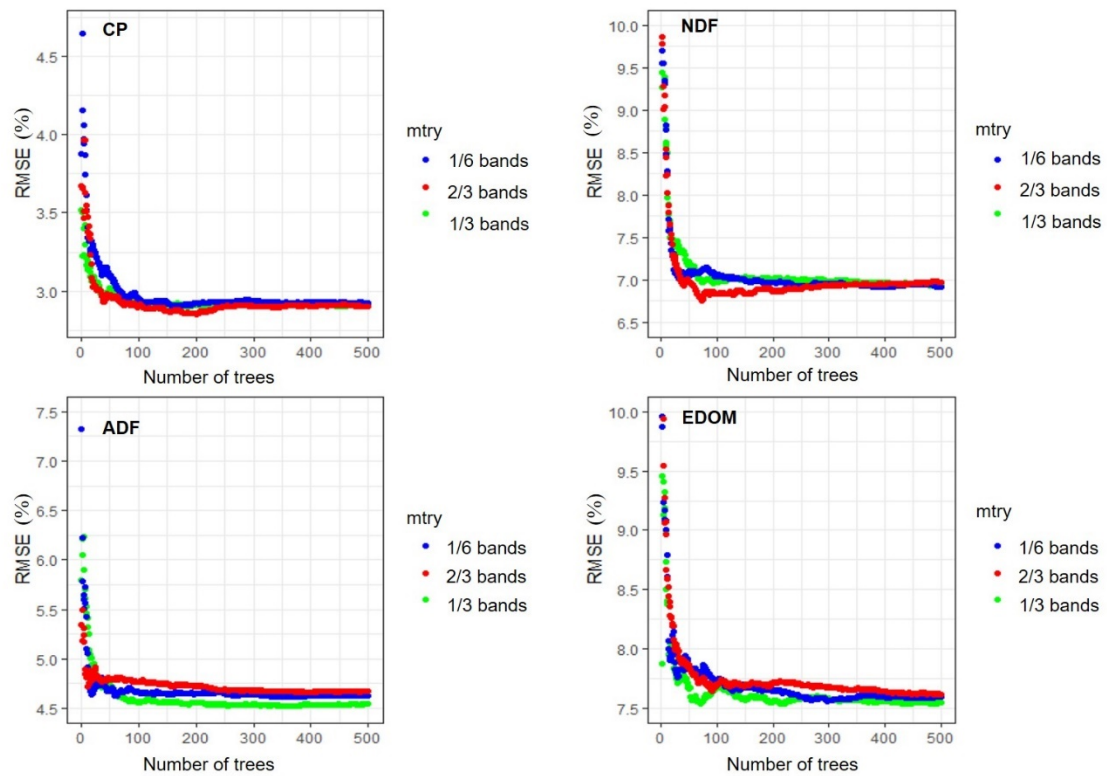
60



61

62 **Fig. S5.** Changes in RMSE of RF models using all bands for each pasture quality
 63 variable with different mtry and ntree values. Default settings are mtry=1/3 and
 64 ntree=500. CP: crude protein; NDF: neutral detergent fibre; ADF: acid detergent fibre;
 65 and EDOM: enzyme digestibility of organic matter.

66



67

68 **Fig. S6.** Changes in RMSE of RF models using the selected bands for each pasture
 69 quality variable with different mtry and ntree values. Default settings are mtry=1/3 and
 70 ntree=500. CP: crude protein; NDF: neutral detergent fibre; ADF: acid detergent fibre;
 71 and EDOM: enzyme digestibility of organic matter.

72

73